2006-09

Propagation modeling of wireless systems on shipboard external decks

Rodriguez Gallo, Luis E.

Monterey California. Naval Postgraduate School

NAVAL POSTGRADUATE SCHOOL

MONTEREY, CALIFORNIA

THESIS

PROPAGATION MODELING OF WIRELESS SYSTEMS ON SHIPBOARD EXTERNAL DECKS

by

Luis E. Rodriguez Gallo

September 2006

Thesis Advisor:	David C. Jenn
Second Reader:	Michael A. Morgan

THIS PAGE INTENTIONALLY LEFT BLANK

REPORT DOCUMENTATION PAGE			Form Approved OMB No. 0704-0188
Public reporting burden for this collection of information is estimated to average 1 hour per response, including the time for reviewing instruction, searching existing data sources, gathering and maintaining the data needed, and completing and reviewing the collection of information. Send comments regarding this burden estimate or any other aspect of this collection of information, including suggestions for reducing this burden, to Washington headquarters Services, Directorate for Information Operations and Reports, 1215 Jefferson Davis Highway, Suite 1204, Arlington, VA 22202-4302, and to the Office of Management and Budget, Paperwork Reduction Project (0704-0188) Washington DC 20503.			
1. AGENCY USE ONLY ***(Leave blank)***	**2. REPORT DATE** September 2006	**3. REPORT TYPE AND DATES COVERED** Master's Thesis	
4. TITLE AND SUBTITLE Propagation Modeling of Wireless Systems on Shipboard External Decks		**5. FUNDING NUMBERS**	
6. AUTHOR Luis E. Rodriguez Gallo			
7. PERFORMING ORGANIZATION NAME(S) AND ADDRESS(ES) Naval Postgraduate School Monterey, CA 93943-5000		**8. PERFORMING ORGANIZATION REPORT NUMBER**	
9. SPONSORING /MONITORING AGENCY NAME(S) AND ADDRESS(ES) N/A		**10. SPONSORING/MONITORING AGENCY REPORT NUMBER**	
11. SUPPLEMENTARY NOTES The views expressed in this thesis are those of the author and do not reflect the official policy or position of the Department of Defense or the U.S. Government.			
12a. DISTRIBUTION / AVAILABILITY STATEMENT Approved for public release; distribution is unlimited		**12b. DISTRIBUTION CODE** A	

13. ABSTRACT

Many on-board ship operations demand full radio coverage over the entire ship, not only indoor, but also from the interior spaces to the other decks. Onboard a ship, specifically in the upper decks, radio wave propagation is subjected to fading that would impede the quality and reliability of data links and communication. One example is the performance of unmanned aerial vehicle (UAV) data and communications links.

The purpose of this thesis is to analyze, model, and simulate some communication scenarios that occur on naval ships using *Urbana*. Starting from known inputs (frequency, ship compartment geometry, material properties, propagation computation model, and antenna type), analytical results reflecting the propagation mechanisms and coverage area are presented. Variable inputs can then be optimized to achieve a desired signal distribution for a specific shipboard environment.

The ship models were created by *Rhino*, a well-known Windows-based computer drawing software. The values of the signals received on the different points in the main deck are computed for different frequencies and powers. The results are used to draw conclusions of the deployment of antennas on the ship as well as operational aspects such as UAV flight paths.

14. SUBJECT TERMS Urbana, Simulation of Wireless Propagation, Outdoor Propagation, Antenna Fundamentals, Radio Wave Propagation, Wireless Networks, Rhino, Matlab.			**15. NUMBER OF PAGES** 81
			16. PRICE CODE
17. SECURITY CLASSIFICATION OF REPORT Unclassified	**18. SECURITY CLASSIFICATION OF THIS PAGE** Unclassified	**19. SECURITY CLASSIFICATION OF ABSTRACT** Unclassified	**20. LIMITATION OF ABSTRACT** UL

NSN 7540-01-280-5500 Standard Form 298 (Rev. 2-89)
Prescribed by ANSI Std. 239-18

THIS PAGE INTENTIONALLY LEFT BLANK

Approved for public release; distribution is unlimited

PROPAGATION MODELING OF WIRELESS SYSTEMS ON SHIPBOARD EXTERNAL DECKS

Luis E. Rodriguez Gallo
Lieutenant, Mexican Navy
B.S., Mexican Naval Academy, 1994

Submitted in partial fulfillment of the
requirements for the degree of

MASTER OF SCIENCE IN SYSTEMS ENGINEERING

from the

NAVAL POSTGRADUATE SCHOOL
September 2006

Author: Luis E. Rodriguez Gallo

Approved by: David C. Jenn
Thesis Advisor

Michael A. Morgan
Second Reader

Dan C. Boger
Chairman, Department of Information Sciences

THIS PAGE INTENTIONALLY LEFT BLANK

ABSTRACT

Many onboard ship operations demand full radio coverage over the entire ship, not only indoor, but also from the interior spaces to the other decks. Onboard a ship, specifically in the upper decks, radio wave propagation is subjected to fading that would impede the quality and reliability of data links and communication. One example is the performance of unmanned aerial vehicle (UAV) data and communications links.

The purpose of this thesis is to analyze, model, and simulate some communication scenarios that occur on naval ships using *Urbana*. Starting from known inputs (frequency, ship compartment geometry, material properties, propagation computation model, and antenna type), analytical results reflecting the propagation mechanisms and coverage area are presented. Variable inputs can then be optimized to achieve a desired signal distribution for a specific shipboard environment.

The ship models were created by *Rhino*, a well-known Windows-based computer drawing software. The values of the signals received on the different points in the main deck are computed for different frequencies and powers. The results are used to draw conclusions of the deployment of antennas on the ship as well as operational aspects such as UAV flight paths.

THIS PAGE INTENTIONALLY LEFT BLANK

TABLE OF CONTENTS

LIST OF FIGURES

LIST OF TABLES

THIS PAGE INTENTIONALLY LEFT BLANK

ACKNOWLEDGMENTS

I would like to express my sincere thanks to Professor David Jenn for his support, guidance, and advice during the research and completion of this thesis. Additional thanks are extended to Professor Michael Morgan for his help and assistance.

Also, I would like to thank my beloved wife, Lucero Scarlet, for her understanding and invaluable support all the time.

THIS PAGE INTENTIONALLY LEFT BLANK

I. INTRODUCTION

A. BACKGROUND

The use of unmanned air vehicles (UAVs) in the U.S. Navy began under former Secretary of the Navy John Lehman, after learning of the Israelis' success using UAVs in Lebanon. The first UAV used by the U.S. Navy was the "Pioneer," but it had limited exposure to operations from ships other than the battleship, and its priority for shipboard operations soon changed with Desert Storm.

By the time Desert Storm began, most of the military tactical reconnaissance capability had been replaced by high resolution satellite imagery. Satellite imagery was collected and transmitted to a controlling ground station for processing and dissemination. Using separate communications links, the developed images were retransmitted to military forces that requested such data. This process proved much too slow and unresponsive to meet the demands of a mobile battlefield, and U.S. military forces found they needed something more timely.

The use of the Pioneer was a very good tool with a capability to collect and transmit real-time imagery during clear weather operations, day or night. Pioneer is shipboard certified and can operate from specifically configured amphibious (LPD-4 class) ships using rocket-assisted launch and vertical net recovery. Despite its limitations, Pioneer proved valuable during Desert Storm.

In February 2000, the Navy awarded Northrop Grumman a contract for Engineering and Manufacturing Development (E&MD) of what became known as the Vertical Take-off and Landing Unmanned Aerial Vehicle (VTUAV). This model offers the best value in consideration of cost, development risk, and capability to meet the desired procurement schedule. The helicopter design is also compatible with all air capable ships [1].

One of the most important missions for these kinds of vehicles is the transmission of images to ground stations. A reliable communication link must be maintained between the UAV and the ship or ground station. The propagation environment is typically very

complex because of shadowing and diffraction. There are areas on deck where the link may drop out. This problem can lead to loss of data or possibly even loss of the UAV if control commands cannot be transmitted.

The proliferation of UAVs is likely to exacerbate one of the biggest problems facing military users of the unmanned reconnaissance tools--managing frequency spectrum.

Late last year, the British Army suffered ten Phoenix UAV mission aborts because interference caused them to lose the command-and-control link. British forces tried to determine the source of the problem, but could never pinpoint it with certainty. Maj. Paul Tombleson believes that a friendly aircraft operating a high-power synthetic aperture radar, using the same frequency as the UAV's command signal, inadvertently jammed the link [2].

This research examines the propagation issues associated with shipboard UAV operations and communications. To simulate this environment in the software package *Urbana* there are some variables that must be selected, such as the antenna pattern, antenna polarization, propagation mechanisms, the materials and their properties, ray launch and bounce options, and the frequency and power of transmission. All of these are variables to be analyzed in this thesis. With all of these inputs the software will produce signal contours which will be analyzed to determine the effect on propagation of the structures present on the main deck of a naval ship.

Also, methods of improving signal coverage in internal spaces of the ship and from the interior to the deck can also be evaluated.

B. OBJECTIVES

The objective of this thesis is to investigate the distribution of power of the signal received onboard the main deck of ships. Methods of improving the propagation characteristics, such as relay antennas, are also examined. In the first case communication with an unmanned aerial vehicle (UAV), for the purposes of this thesis an RQ-8B Fire Scout Vertical Takeoff and Landing Tactical UAV System (VTUAV) and a DDG-51

ARLEIGH BURKE-class ship, is simulated. The simulation duplicates the complex propagation environment in which the UAV operates. Testing and evaluation of these values were conducted using the commercial software package *Urbana*. In the second case a cargo ship is simulated and an antenna is placed at different places near the bridge to analyze the best position for complete coverage over the entire main deck.

C. RELATED WORK

In [2] Sumagasay used *Urbana* to analyze Wireless Local Area Network (WLAN) signal distribution in single story and high-rise buildings at a frequency of 2.4 GHz. In [4] Boukraa concluded that the signal levels for a 1 Watt transmitter could only be detected at the -70 dBm level within two floors of a high-rise structure.

In [5] Kaya also used this software to simulate wireless propagation and jamming in a high-rise building, and Chaabane studied the propagation characteristics of Wide Local Area Networks (WLANs) in ship spaces. Several other theses have modeled propagation in dense urban environments [6, 7, 8]. This thesis makes use of many of the tools developed in these early projects.

D. THESIS OUTLINE

This thesis is divided into five chapters. Chapter II is an overview of antenna propagation fundamentals. A description of the software used in this analysis, *Rhino* and *Urbana*, is presented in Chapter III. The simulation setup and results are described in Chapter IV. Lastly, conclusions and future work are presented in Chapter V.

THIS PAGE INTENTIONALLY LEFT BLANK

II. BACKGROUND

This chapter explains how electromagnetic (EM) waves propagate and introduces important background information that relates to wireless propagation. Also discussed are the fundamentals of antenna theory, and the key principles of EM propagation such as attenuation in bulk materials, scattering, and interference.

A. PHYSICS OF PROPAGATION

1. Electromagnetic Radiation

Electromagnetic radiation consists of simultaneously oscillating electric and magnetic fields that are coupled as described by Maxwell's equations:

$$\nabla \times \vec{E} = -\frac{\partial \vec{B}}{\partial t}, \tag{1.1}$$

$$\nabla \times \vec{H} = \frac{\partial \vec{D}}{\partial t} + \vec{J}, \tag{1.2}$$

$$\nabla \cdot \vec{D} = \rho, \tag{1.3}$$

$$\nabla \cdot \vec{B} = 0, \tag{1.4}$$

where $\vec{E}$ (V/m) is the electric field intensity, $\vec{D}$ (C/m^2) is the electric displacement, $\vec{B}$ (T) is the magnetic flux density, $\vec{H}$ (A/m) is the magnetic field intensity, ρ (C/m^3) is the charge density, and $\vec{J}$ (A/m^2) is the current density. From this point, one assumes time-harmonic fields with a $e^{j\omega t}$ time dependence and uses phasor notation.

Maxwell's equations provide us with the relationship between electric and magnetic fields, as well as sources that give rise to the fields, and allow determining the way in which these fields (radio waves) interact with the environment [15].

Before proceeding, it is necessary to introduce the material constitutive parameters that relate the field intensities to the flux densities:

$$\vec{D} = \varepsilon \vec{E}, \tag{1.5}$$

$$\vec{B} = \mu \vec{H}, \tag{1.6}$$

$$\vec{J} = \sigma \vec{E}, \tag{1.7}$$

where ε, μ and σ are, respectively, the permittivity, permeability and conductivity of the medium through which the waves are propagating. Complex ε and μ, along with σ, completely describe a linear, time invariant material:

$$\mu = \mu_0 \mu_r = \mu_0 (\mu_r' - j\mu_r''), \tag{1.8}$$

$$\varepsilon = \varepsilon_0 \varepsilon_r = \varepsilon_0 (\varepsilon_r' - j\varepsilon_r''), \tag{1.9}$$

where $\mu_o = 4\pi \times 10^{-7}$ (A/m) and $\varepsilon_0 = 8.8542 \times 10^{-12}$ (F/m) is the free-space permittivity. The intrinsic impedance of the medium is:

$$\eta = \sqrt{\frac{\mu}{\varepsilon}}. \tag{1.10}$$

Assuming that the region of space of interest is source free (charge density and current density are zero), Maxwell's equations can be solved to yield the wave equation for the electric field:

$$\nabla^2 \vec{E} + k^2 \vec{E} = 0, \tag{1.11}$$

where $k = \omega\sqrt{\mu\varepsilon} = 2\pi/\lambda$, $\omega = 2\pi f$, f is the frequency, and λ is the wavelength that is equal to:

$$\lambda = \frac{c}{f}. \tag{1.12}$$

The most elementary solutions of the wave equation are plane waves:

$$\vec{E} = \vec{E}_0 e^{\pm j\vec{k}\cdot\vec{r}}, \tag{1.13}$$

where $\vec{E}_0$ is a complex constant, $\vec{k}$ is a vector in the direction of propagation, and $\vec{r}$ is a position vector form the origin to the point (*x,y,z*) where the electric field is evaluated. [10]

The wave equation admits other solutions, among them are spherical waves. A uniform spherical wave may be represented, for example, as:

$$\vec{E} = E_0 \frac{e^{-jkr}}{r} \hat{\theta}, \tag{1.14}$$

As is illustrated in Equation (1.14), the electric field strength falls off inversely with the radial distance r from the point where propagation is initiated. The power carried by the wave spreads as $1/r^2$ (the inverse square law). In addition, the wave is also subject to attenuation (energy dissipated inside a material) and scattering as it interacts with objects. It can also interact with other waves through the process of interference (superposition).

2. Attenuation of Electromagnetic Radiation in Bulk Materials

As waves propagate through a lossy medium, energy is extracted from the wave and absorbed by the medium. The three main sources of loss are ohmic loss (due to the collision of free charges in a conductor), dielectric loss (due to the polarization of molecules caused by an external electric field), and magnetic loss (due to the magnetization of the molecules caused by an external magnetic field) [14].

The time-averaged power density of the spherical wave is:

$$\overline{W} = \frac{1}{2} \mathrm{Re}\left\{ \vec{E} \times \overline{H}^* \right\} = \frac{|E|^2 \hat{r}}{2\eta} = \frac{|E_0|^2}{2\eta} \frac{e^{-2\alpha r}}{r^2} \hat{r}, \tag{1.15}$$

where E_0 is the field at the reference and α is the field attenuation coefficient that determines the rate of decay of the wave. The value of the attenuation coefficient has been tabulated for different materials at different wavelengths and it can be calculated from the constitutive parameters of the medium.

3. Scattering Mechanisms

When an incident electromagnetic wave impinges onto a surface of a material or meets an obstacle, it can either go through it after a process of refraction which leads to a transmitted wave along with scattering. The main scattering mechanisms that are encountered in an ship environment are shown in Figure 1.

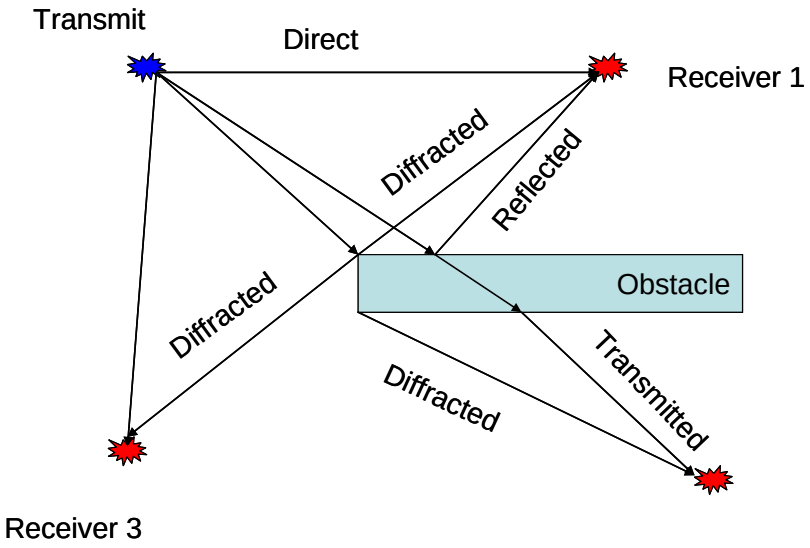

Figure 1. Scattering mechanism.

a. Reflection and Transmission

When an electromagnetic wave is incident on an interface between two media with different characteristics, some of the radiation is reflected by the interface, while some is transmitted through it. The direction of propagation of the transmitted wave is altered through a process called refraction. For a panel in free-space, by Snell's Law, the reflected wave leaves the interface at the same angle θ_i relative to the normal as the incident wave arrives. The angle of the transmitted wave is:

$$\sin\theta_t = \frac{n_1}{n_2}\sin\theta_i, \tag{1.16}$$

where n_1 and n_2 are the refractive indices of the two media as shown in Figure 2. The index of refraction for a medium n is:

$$n = \sqrt{\varepsilon_r \mu_r}\,. \tag{1.17}$$

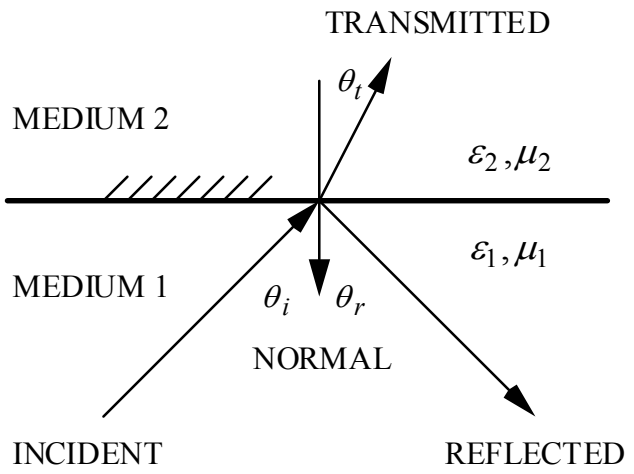

Figure 2. Reflected and transmitted waves.

The amplitude of the wave reflected from a perfect electric conductor (PEC) suffers no reduction as none of the energy is transmitted. For dielectrics, the reflection coefficient is:

$$\Gamma = \frac{n_1 - n_2}{n_1 + n_2}, \tag{1.18}$$

This coefficient relates the incident and reflected fields:

$$E_r = \Gamma E_i. \tag{1.19}$$

b. Diffraction

Diffracted waves are those scattered from discontinuities such as edges and tips. Although most diffracted waves are less intense than reflected waves, they can scatter over a wide range of angles. Because these diffracted waves carry electromagnetic energy in many directions, they make it possible for waves to reach shadow areas that neither direct nor reflected waves could reach. Similar to the case of reflection, a diffraction coefficient, *D*, can be defined that relates the incident and diffracted fields:

$$E_d = DE_i. \tag{1.20}$$

Formulas are available for computing D for various discontinuities [10].

4. Interference

Two electromagnetic waves can interfere with each other. The amplitude at any point in space is equal to the peak absolute value of the total local electric field. The total field at an observation point is the sum of all direct, scattered (reflected and diffracted) and transmitted fields arriving at that point. Because the local field is the vector sum of all electric fields reaching that point from all contributing sources, the intensity of the electromagnetic radiation can vary greatly depending on the location of the point with respect to other emitting sources. Interference can lead to signals higher than the direct path component when EM waves reinforce, and to very low signal levels when they cancel (fading). This is a crucial problem for naval ships where sources of interference are everywhere for all frequency bands.

B. ANTENNA FUNDAMENTALS

Antennas are the part of a transmitting and receiving system. They are designed to radiate and to receive electromagnetic waves [12]. In doing so, they perform three main functions:

1) Provide a match between the impedance of the transmission line, waveguide or any other connecting device, and the impedance of the space where they are emitting or sensing.

2) Provide gain relative to an isotropic radiator by collimating or collecting the radiation into a beam that focuses the EM energy.

3) Provide a means of pointing the beam in specific directions (scanning).

Antennas perform these tasks both when transmitting as well as when receiving [12].

1. Antenna Gain

The gain of an antenna is a measure of the ability, in terms of relative power, of the antenna to focus radio waves in a particular direction as compared to an isotropic reference element. In practice, the gain of an antenna can be determined from its effective area, A_e, and the wavelength λ by:

$$G = \frac{4\pi A_e}{\lambda^2}. \tag{1.21}$$

For an efficient antenna with a well-defined physical aperture area, A, one can use $A_e \approx Ae$ where e is the antenna efficiency (the ratio of power radiated to that input).

2. Antenna Polarization

The antenna polarization refers to the vector direction of the wave radiated by the transmitting antenna in terms of the time-varying orientation of the electric field. The tip of the electric field vector traces a path in space, and in the most general case it is elliptical. This is called *elliptical polarization.* If the path is a circle or a straight line, then the polarization is called *circular* or *linear,* respectively.

In most wireless applications, the transmitting and the receiving antennas are linearly polarized. Polarization mismatch loss occurs if the transmitting and receiving antennas are not similarly polarized, or not aligned. Polarization loss can be a significant problem for UAV links when a linear polarized antenna is used.

3. Antenna Pattern Characteristics

The radiation pattern represents the antenna's radiated (or received) power as a function of an angle at a fixed radius from a receiving (or transmitting) antenna. When receiving, an antenna responds to an incoming wave from a given direction according to the pattern value in that direction. Figure 3 [13] illustrates some important antenna pattern characteristics. The figure shows the antenna main lobe, the half power beam width defined at the half-power points and the beam width between fist nulls.

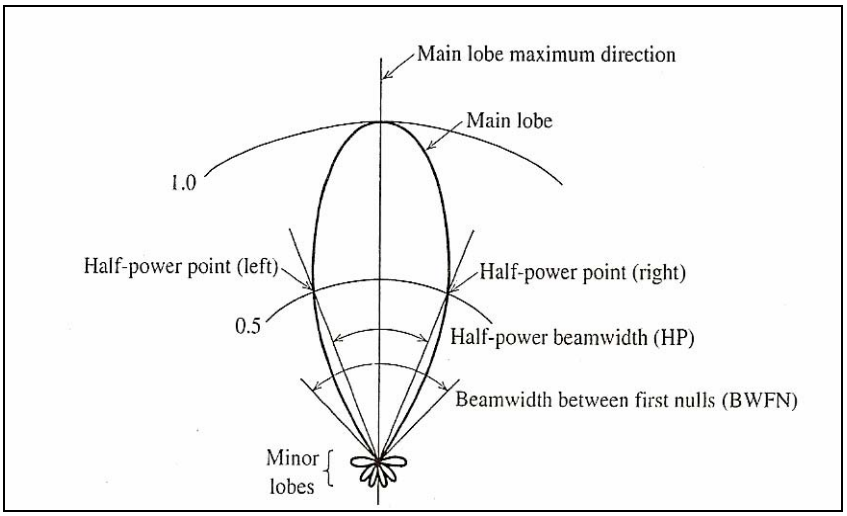

Figure 3. A typical power pattern polar plot. (From Ref. [13])

A vertical half-wave dipole antenna, which has an omni-directional pattern in the horizontal plane, is the most common omni-directional antenna of choice. Parabolic type reflectors or arrays are used when it is necessary to direct the transmitted energy into a specific direction with a narrow beam. In this thesis, two antenna types are used: a short dipole and a uni-directional antenna.

C. FREE-SPACE LINK EQUATION

Assuming no polarization mismatch loss and no obstruction between the transmitting and the receiving antennas, as shown in Figure 4, the received signal power in free-space can be expressed by Friis's transmission formula [13]:

$$P_r = \frac{P_t G_t G_r \lambda^2}{(4\pi d)^2}, \tag{1.22}$$

where P_t is the transmitted power in watts, d is the distance between the transmitting and the receiving antennas, and G_t and G_r are the gains of transmitting and the receiving antennas, respectively.

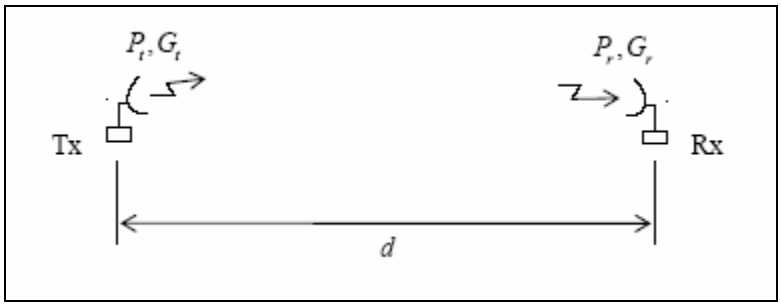

Figure 4. A free-space communication link

The *effective isotropically radiated power* (EIRP) is the transmitted power into the antenna multiplied by the power gain of the transmitting antenna in a given direction relative to an isotropic antenna:

$$EIRP = P_t G_t, \tag{1.23}$$

and it is often called the *effective radiated power* (ERP). For convenience, the free-space link equation is written in decibels:

$$P_r = P_t + G_t + G_r - (L_{fs} + L)\,[\text{dB}], \tag{1.24}$$

where L_{fs} and L are the free-space path loss and the other losses, respectively. The free-space path loss is proportional to the inverse square of the distance between transmitting and receiving antennas and is frequency dependent:

$$L_{fs} = 10\log\left(\frac{4\pi d^2}{\lambda^2}\right)[\text{dB}]. \tag{1.25}$$

D. GEOMETRIC OPTICS

Geometrical optics (GO) refers to the simple ray-tracing techniques that have been used for centuries at optical frequencies. The basic postulates of GO are:

1. Wave fronts are locally plane and waves are TEM.

2. The wave direction is specified by the normal to the equiphase planes ("rays").

3. Rays travel in straight lines in a homogeneous medium.

4. Polarization is constant along a ray in an isotropic medium.

5. Power in a flux tube ("bundle of rays") is conserved (Figure 5).

$$\iint_{Area1} \vec{W} \cdot d\vec{s}_1 = \iint_{Area2} \vec{W} \cdot d\vec{s}_2 . \tag{1.26}$$

6. Reflection and refraction obey Snell's law.

7. The reflected field is linearly related to the incident field at the reflection point by a reflection coefficient.

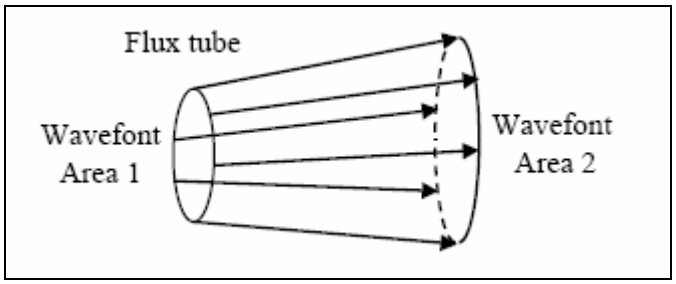

Figure 5. Flux tube (From Ref. [13])

Disadvantages of GO is that it:

1. Does not predict the field in shadows, and

2. Cannot handle flat or singly curved surfaces.

E. THE GEOMETRICAL THEORY OF DIFFRACTION

The geometrical theory of diffraction (GTD) was developed to improve on the GO approximation by adding edge-diffracted fields. Such diffracted rays operate as a secondary source of energy. The total field at a point in space is the sum of all reflected, direct, and diffracted fields arriving at that point. Formulas are available to compute the diffraction from an edge [14].

The diffracted field is linearly related to the incident field at the diffraction point by a diffraction coefficient. The diffraction coefficient is dependent upon the angle of incidence onto the edge, the incident polarization, the wedge angle of the surfaces

forming the edge, and the type of material. The diffracted ray trajectory lies on the surface of cone, which has a half-angle equal to the angle of incidence of the wave with the edges (Figure 6).

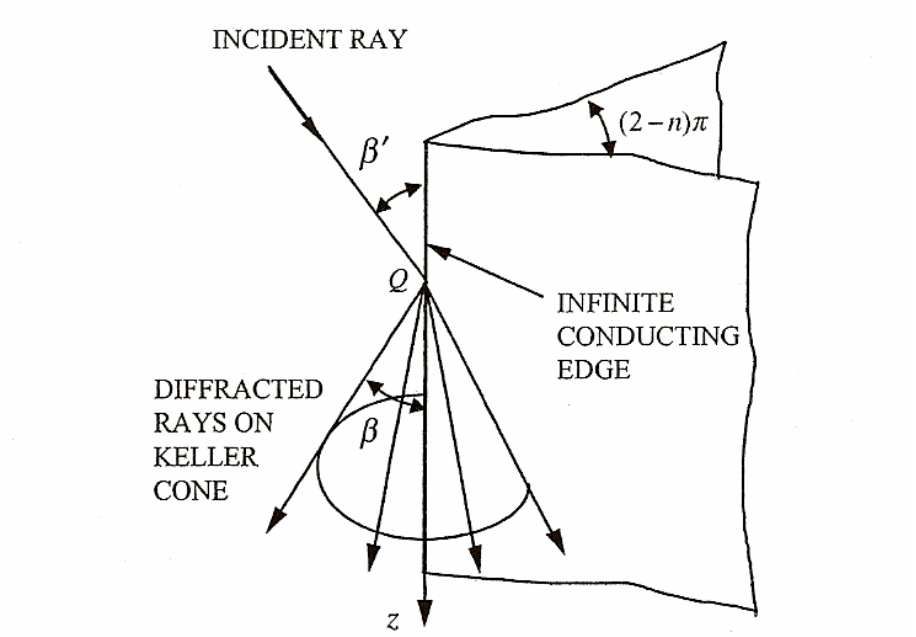

Figure 6. Diffracted ray geometry and the Keller cone. (From Ref. [13]).

The strongest diffracted fields arise from edges, but ones of lesser strength originate from point discontinuities (tips and corners). The total field at an observation point *P* is decomposed into GO and diffracted components [14]:

$$\overrightarrow{E_r}(P) = \vec{E}_{GO}(P) + \vec{E}_{GTD}(P). \tag{1.27}$$

The behavior of the diffracted field is based on the following postulates of GTD:

1. Wave fronts are locally plane and waves are TEM.
2. Diffracted rays emerge radially from an edge.
3. Rays travel in straight lines in a homogeneous medium.
4. Polarization is constant along a ray in an isotropic medium.

5. The diffracted field strength is inversely proportional to the cross sectional area of the flux tube.

6. The diffracted field is linearly related to the incident field at the diffraction point by a diffraction coefficient [14].

Many commercial software packages are available to compute the total field by summing the direct, reflected and diffracted components arriving at the point. There are also higher order contributions that may be important: multiple reflections, multiple diffractions, reflected-diffracted, diffracted-reflected, etc. Usually the multiple diffractions and mixed terms can be neglected. For this research, *Urbana* was selected as the modeling tool. Its capabilities are discussed in the next chapter.

III. PROPAGATION MODELING USING URBANA

A. RAY TRACING WITH URBANA

The ray tracing software, *Urbana,* from Science Applications International Corporation (SAIC), was used to model and simulate the effects of the structures on the upper decks onboard different kinds of ships. This chapter describes the capabilities of *Urbana* and how the simulation models were constructed.

Urbana is a powerful computational electromagnetic (CEM) tool for simulating wireless propagation in complex environments utilizing a ray tracing engine that combines physical optics, geometric optics, and diffraction physics to produce a 3-D simulation [14]. *Urbana* applies ray tracing to CAD models for buildings, and major structures like ships. At a basic level, the ray tracer is used to interrogate the 3-D geometry of the environment to provide requisite inputs to any number of physical models for reflection, diffraction around buildings, diffraction around terrain, etc.

For radio wave propagation modeling, the input parameters for *Urbana* are CAD facet models for the ships and the sea surface, including its surface material (e.g., sea water, PEC, glass and dielectrics). The other inputs are the placement, strength, and antenna patterns of transmitters. The outputs are composite signal strength, angle of arrival and time delay of each arriving signal ray at each receiver or observation point. For wireless applications, users specify the observation coverage regions that conform to the terrain and buildings in the scene, and *Urbana* computes the field level at each duplicate receiver or coverage region sampling point.

Urbana permits the study of different antenna designs and the use of different locations to determine the best configuration for a specific application.

B. SOFTWARE USED TO CREATE THE MODELS

1. CAD

Computer Aided Design (CAD) is used to design and develop products, which can be goods used by end consumers or intermediate goods used in other products. CAD

is also extensively used in the design of tools and machinery used in the manufacture of components. CAD is also used in the drafting and design of all types of buildings, from small residential types (houses) to the largest commercial and industrial types (hospitals and factories) [12].

CAD is used throughout the engineering process from conceptual design and layout, to detailed engineering and analysis of components, to definition of manufacturing methods.

In this thesis, the geometry files are based on several CAD models available on the web page http://www.3dcadbrowser.com/ [13]: a DDG Arleigh Burke-Class frigate, a RQ-8B Fire Scout Vertical Takeoff and Landing Tactical UAV System (VTUAV) and a cargo ship. Figures 7 through 9 show the CADs models used.

Figure 7. RQ-8B Fire Scout CAD model.

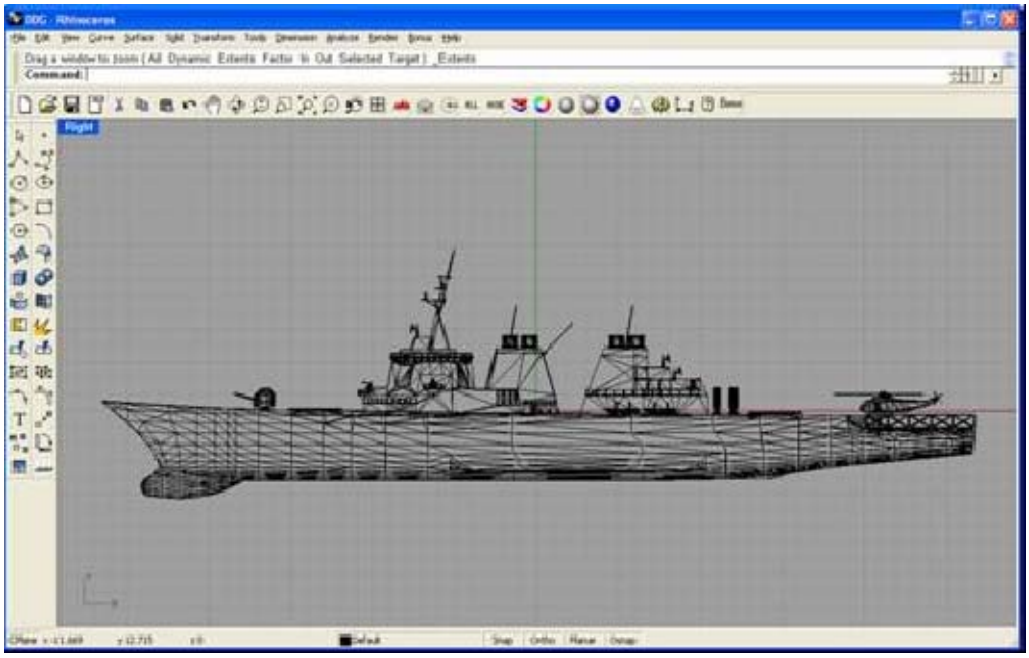

Figure 8. DDG CAD model.

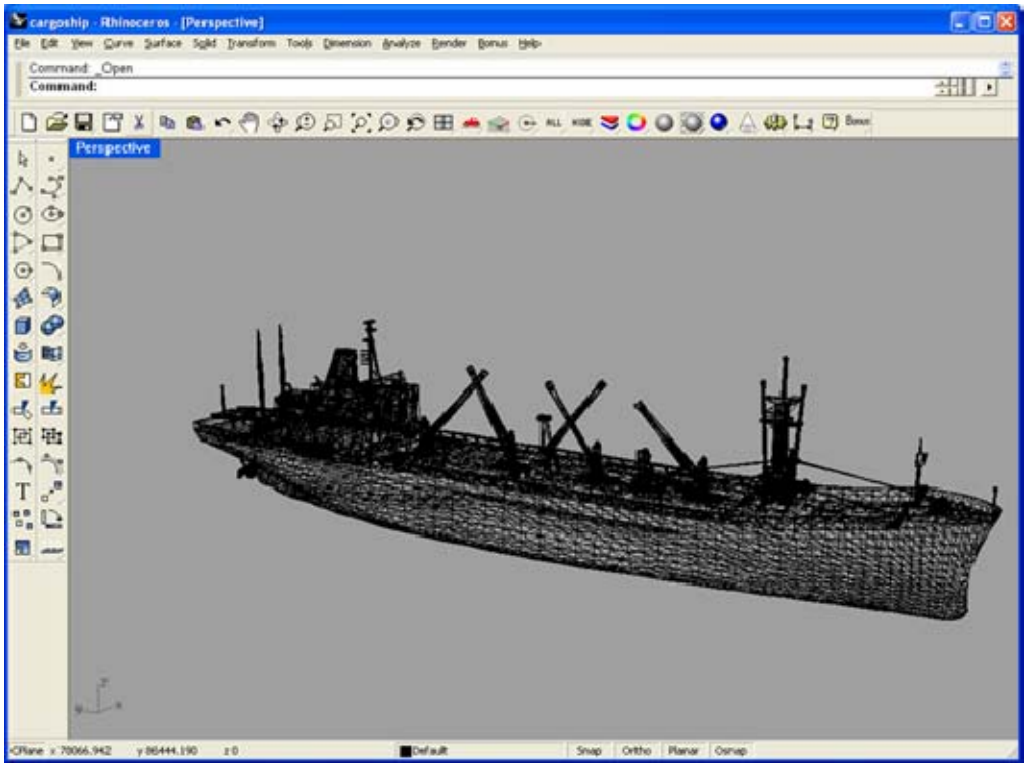

Figure 9. Cargo Ship CAD model.

2. RHINO

Rhino is a very powerful Computer Aided Design (CAD) software package for Windows platforms, and is an uninhibited free-form, 3-D, Non-Uniform Rational B-Spline (NURBS) modeling tool that can model arbitrary shapes. *Rhino* can create, edit, analyze and translate curves, surfaces and solids. Not complex to use, or limited by the degree or size of the environment under study, *Rhino* is well-suited to the design of prototypes and is compatible with most drawing programs. *Rhino*'s features include a file format that supports **.3ds, *.iges,*.dwg, *.vrml, *.bmp, *.jpg* and others.

The reason for using *Rhino* for this thesis is to transform the CAD models obtained off the web page http://www.3dcadbrowser.com/ to the **.facet* format that is required as an input to *Urbana*. Facets are simply triangles that have been stitched together to form surfaces. Facetted geometry representations are commonly used for graphics, bio-medical, geotechnical and many other applications that output a discrete surface representation [14]. The translation process is performed using the *Menelaus* application.

Menelaus 3D is a console program comprised of a set of smaller, single purpose utilities. These tools form basic building blocks which may be invoked singly or in sequence to perform manipulations on facet and edge geometry files. *Rhino* is used to save CAD models in **.3ds* format. After that the *Menelaus* file translator is used to transform **.3ds* files to **.facet* files, to be used as an input file in *iUrbana*, the graphical user interface for *Urbana*.

Menelaus 3D is used to extract edges (**.edge*) from the facet file. *Urbana* requires a set of observation points at which the field is to be computed. To build an observation point list, a *Matlab* script file (shown in Appendix A), is run and the output file is saved in ASCII **.txt* format. In addition, *Urbana* requires the user to set the antenna patterns and polarization, base station location, electromagnetic (EM) parameters, and finally to set the format of the output and results.

C. PROCEDURE TO USE URBANA ON THE PC

The process for running *Urbana* is depicted in Figure 10. The steps are described briefly below.

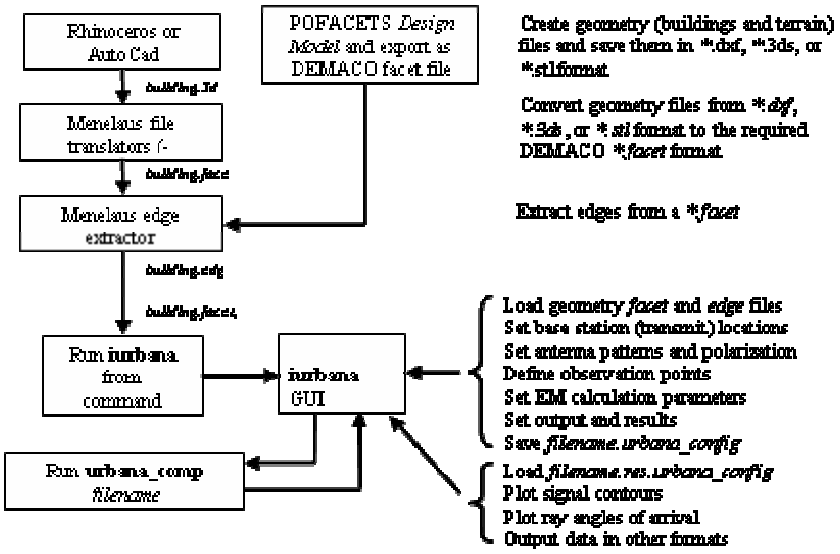

Figure 10. Diagram of the *Urbana* process.

1. Introducing Data in the Graphical User Interface (GUI) (Step 1)

Urbana consists of two major parts: *iUrbana* and *Urbana_comp*. *iUrbana* is the front-end application providing a GUI for a user to introduce the data. This GUI has two main tabs to introduce the data necessary to run *Urbana*.

The first tab is named **Scenario**. It contains the **Environment** dialog that is used to specify the CAD model and its materials for the scene in facet format. The **Scenario** tab includes the terrain (including buildings), antenna elements, base stations and coverage regions.

The **Environment** dialog is also used to specify an optional edge model. This is typically for building edges and allows the computational engine to predict edge diffraction.

There is also an **Analysis** tab, which controls the various computation factors such as which base station to use, how to calculate the propagation, what to do with the results, etc.

Finally, there is a **Results** tab that specifies how the results are to be formatted and presented.

After all this data is introduced the file is saved as an **.urbana_config* file.

2. Run Urbana (Step 2)

The *Urbana* input file (**.urbana_config*) is composed of the key input parameters and the file names described above, and the *urbana_comp* command is run at the command prompt (DOS window). After executing *Urbana*, the output is summarized in a **.res.urbana_config* file.

3. Post Processing (Step 3)

Finally, with the **.res.urbana_config* file loaded into *iUrbana,* the results are displayed from the **Scenario** and **Results** dialog, as shown in Figure 11.

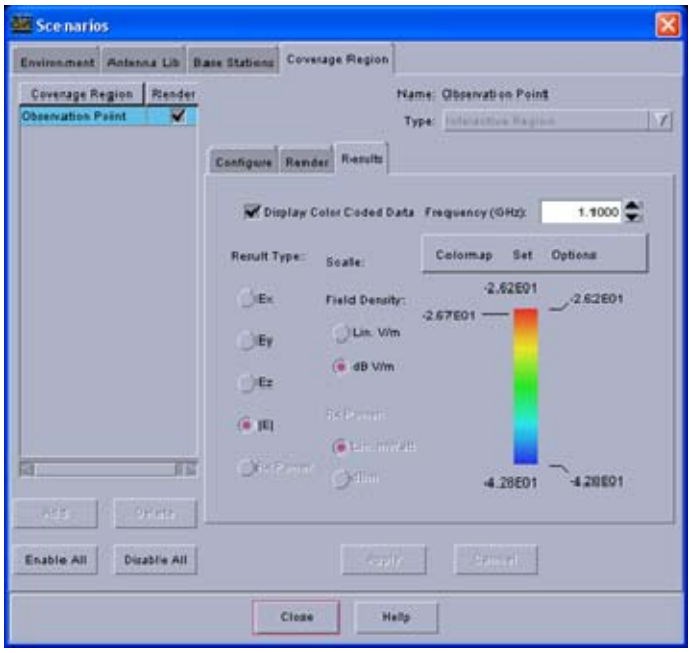

Figure 11. Result dialog.

A color bar is shown in Figure 11. It is composed of a continuous range of colors between blue and red, representing the variation of the signal strength level between the minimum and maximum values throughout the coverage region established. Figure 12 shows an example of an *Urbana* output.

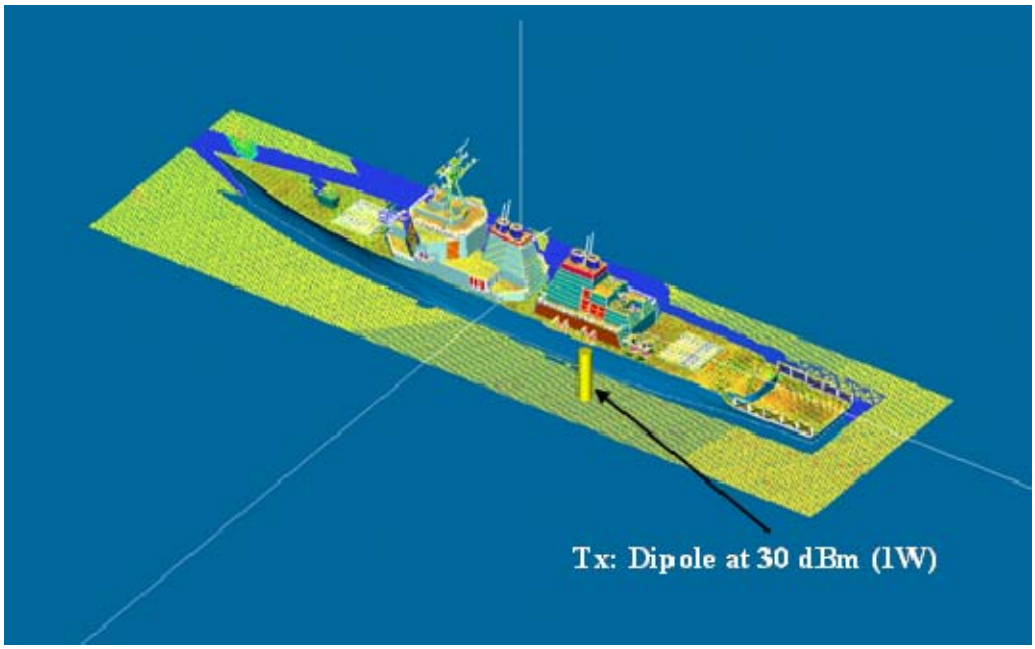

Figure 12. Example of *Urbana* output results.

The *Urbana* model allows the user to understand the frequency dispersive properties of a channel introduced by realistic materials. The procedure for using *Urbana* to generate signal contours has been discussed. In the next chapter the ship simulation data is presented.

THIS PAGE INTENTIONALLY LEFT BLANK

IV. URBANA SIMULATIONS, ANALYSIS AND RESULTS

The previous chapter described the software that can be used to build a scenario where the UAV is using an antenna to transmit information to a DDG Frigate ship. It also and gave a brief introduction to propagation modeling. This chapter describes the antenna and the platform properties, the different positions of the antenna and the evaluation of the results.

A. ANTENNA MODELS

Two different antenna patterns were used in this thesis; both were created using a *Matlab* code named *MakeAntennaFile.m*, which is presented in Appendix B. The main characteristics of the antennas are presented in Table 1. Selected patterns are shown in Figures 13 through 18. In calculating the signal contours the magnitude of the electric field is used:

$$|E| = \sqrt{|E_\theta|^2 + |E_\varphi|^2} \tag{4.1}$$

Parameter	Unidirectional	Dipole
Frequency	*2.4* GHz	*2.4* GHz
Orientation	*z* normal	*z* directed
HPBW	*60*	*78°*
Directivity	*9.3502*	*1.6*
Directivity in dB	*9.7082* dB	*2* dB

Table 1. Characteristics of the antennas.

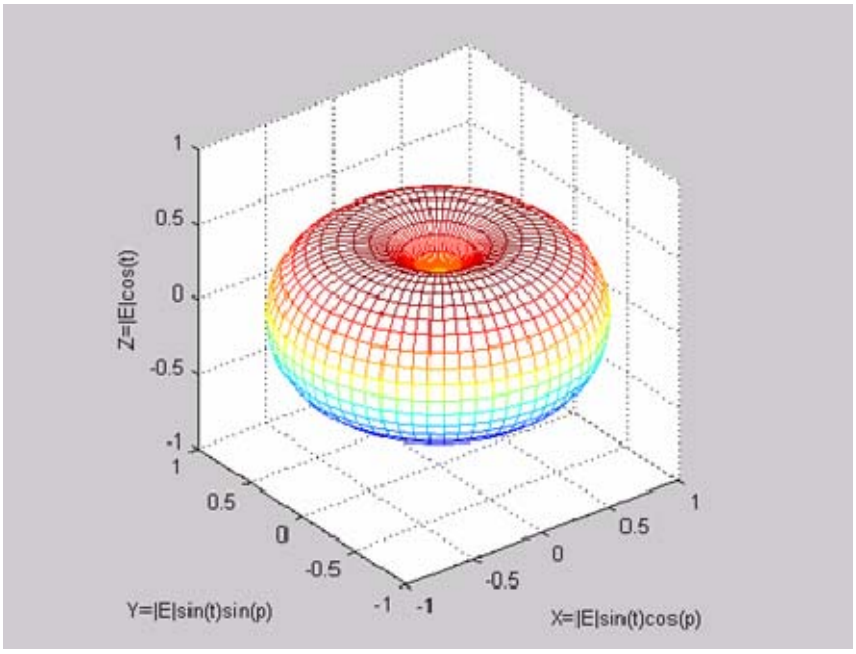

Figure 13. The 3-dimensional radiation pattern of a dipole antenna. The dipole is parallel to the *z* axis.

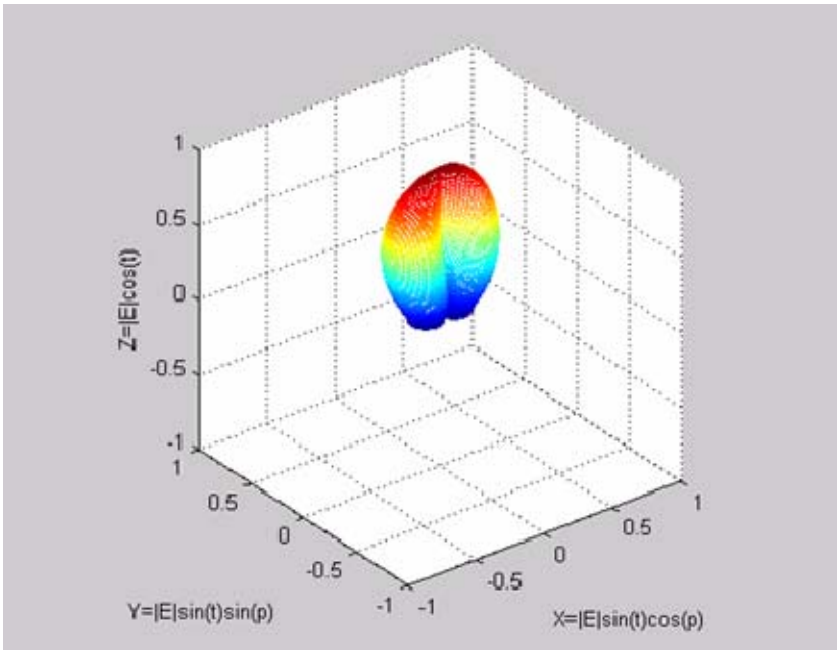

Figure 14. Three dimensional E_θ radiation pattern of the directional antenna.

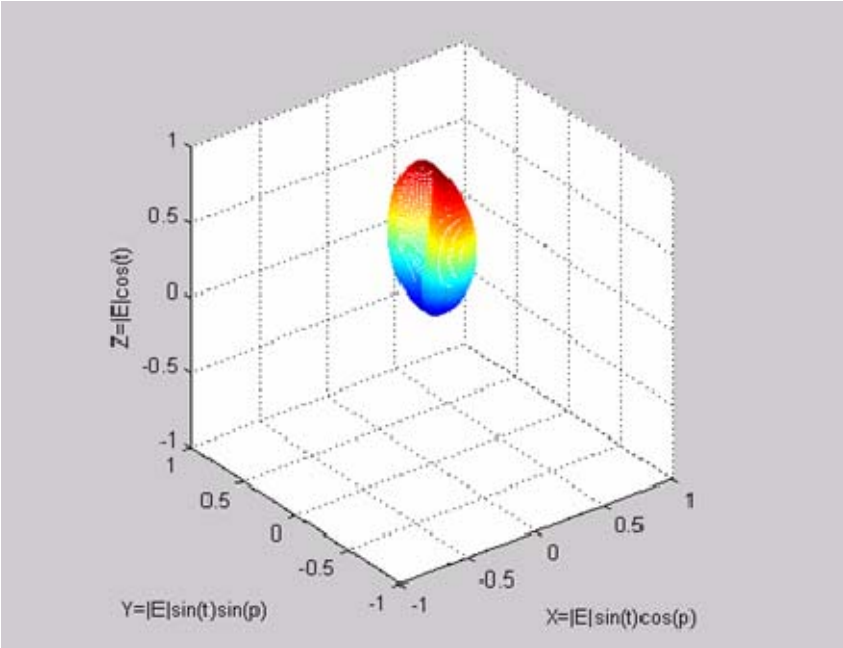

Figure 15. Three dimensional E_φ radiation pattern of the directional antenna.

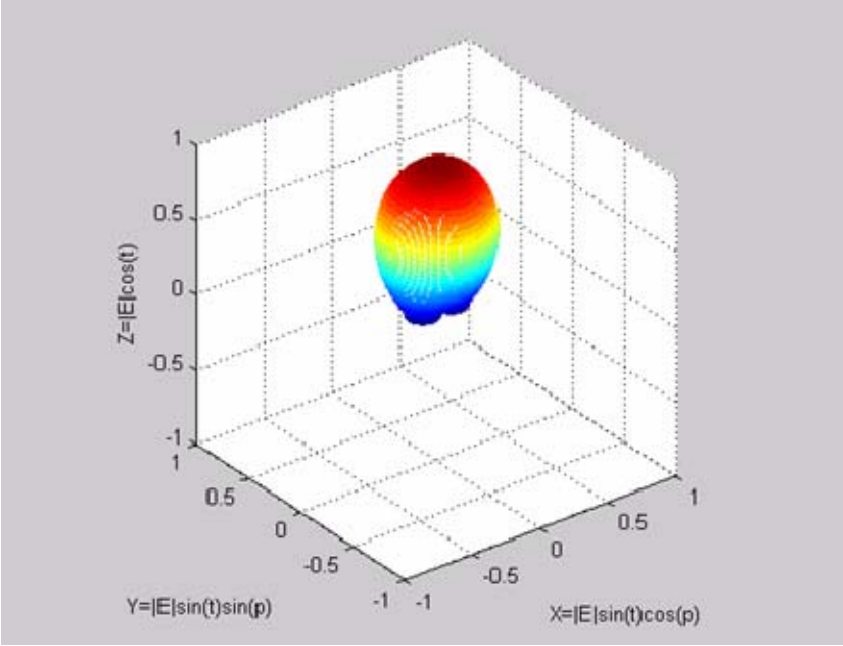

Figure 16. Three dimensional combined E_θ and E_φ radiation pattern of the directional antenna.

In the simulations, the transmitter antenna is located on the exterior part of the UAV. There are two different positions: one with horizontal polarization under the fuselage looking down as shown in Figure 17; and the second position with vertical polarization in the front looking forward as shown in Figure 18.

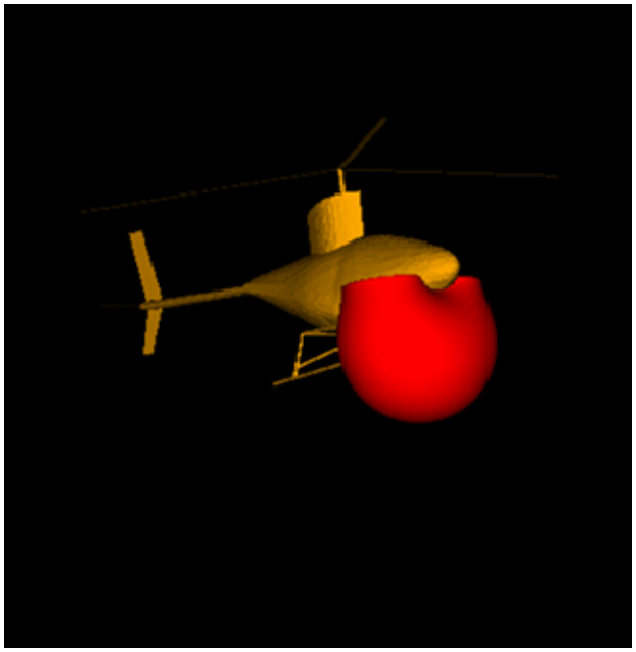

Figure 17. Dipole antenna installed under the UAV.

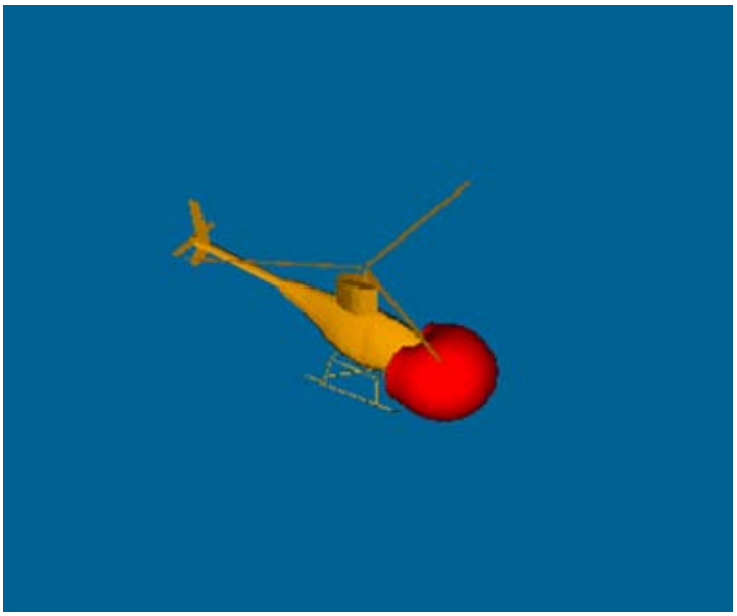

Figure 18. Dipole antenna installed in front of the UAV.

The characteristics of the transmitting and receiving antennas are essential parameters for *Urbana* processing. Basically, different types of antennas affect radio wave propagation differently through their radiation patterns.

1. Antenna File

For *Urbana*, an antenna pattern file containing the linear field strength components of the antennas was created. The pattern file is generated using the *Matlab* code shown in Appendix B. The pattern is normalized to the directivity, which is automatically computed by *Urbana*.

2. Materials

The material selected to build the UAV, the ships and the ground plane is perfect electric conductor (PEC), which is an idealization of a good conductor such as some highly conducting metal or dielectric of very high permittivity. It can be defined as a material in which $\vec{E}_{\tan} = 0$ at the surface. The material properties are shown in Table 2.

COATING MATERIALS	*Material*	*ICOAT*	*Permeability* (μ', μ'')	*Permittivity* $(\varepsilon', \varepsilon'')$	*Resistivity* (Ohms)	*Thickness* (meters)
DDG Ship, UAV and ground plane	*Metal*	*0(PEC)*	(1,0)	(1,0)	0	0.05
Windows in Cargo Ship	*Glass*	*0(PEC)*	(1,0)	(3,0)	0	0.05

Table 2. Properties of materials.

In the scenario of the cargo ship, as in the UAV and DDG ship, the hull and the ground plane are built with PEC material. The cargo ship was modified to transform all the portholes and the windows in the bridge to glass material, as shown in red in Figure 19.

ICOAT is an *Urbana* designation for materials. For each ICOAT value there is an associated μ and ε.

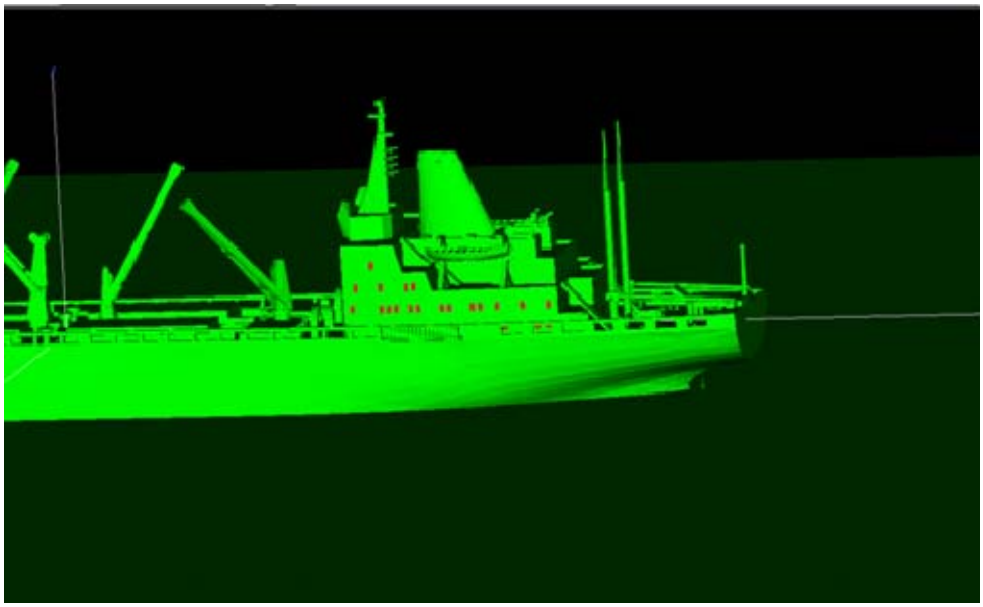

Figure 19. Aft section of the cargo ship showing glass windows.

3. Ground Plane

A large ground plane is included with the ship models to represent the ocean surface. The DDG model and ground plane are shown in Figure 20. The ground plane size is large enough so that the UAV and ship are over the ground plane for all UAV locations. The ground plane cuts through the hull at the water line.

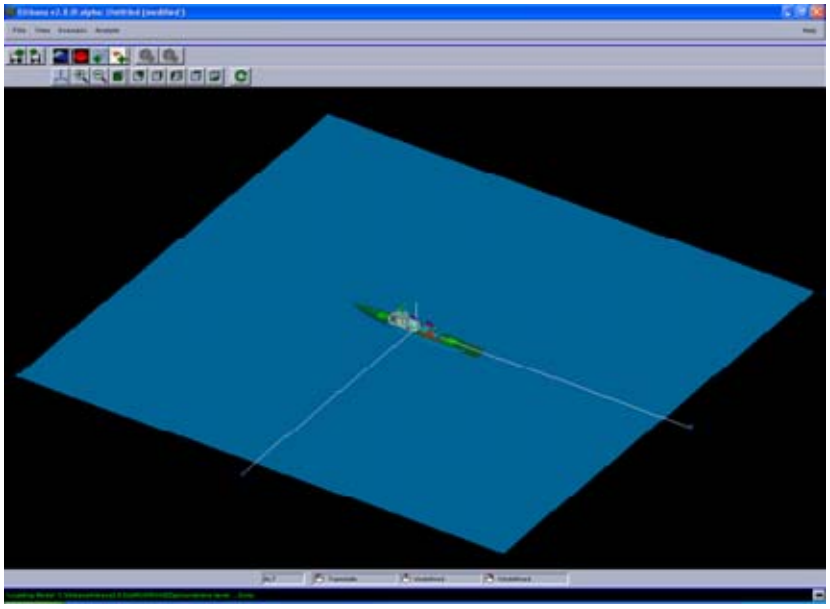

Figure 20. DDG ship and ground plane representing the ocean surface.

4. UAV Positions

To analyze the effect of the structures on the main deck on the propagation, three different positions of the UAV with respect to the DDG ship were used. Figures 21, 22, and 23 show the different positions. Table 3 shows the coordinates of the UAV. All the values are in meters. The UAV is in straight and level flight and pointed as indicated in Table 3.

POSITION	x	y	z	Direction
ONE	**30**	**-50**	**20**	**+ y**
TWO	**30**	**0**	**20**	**+ y**
THREE	**0**	**70**	**20**	**- y**

Table 3. Coordinates of the three positions of the UAV with respect to the DDG Frigate Ship.

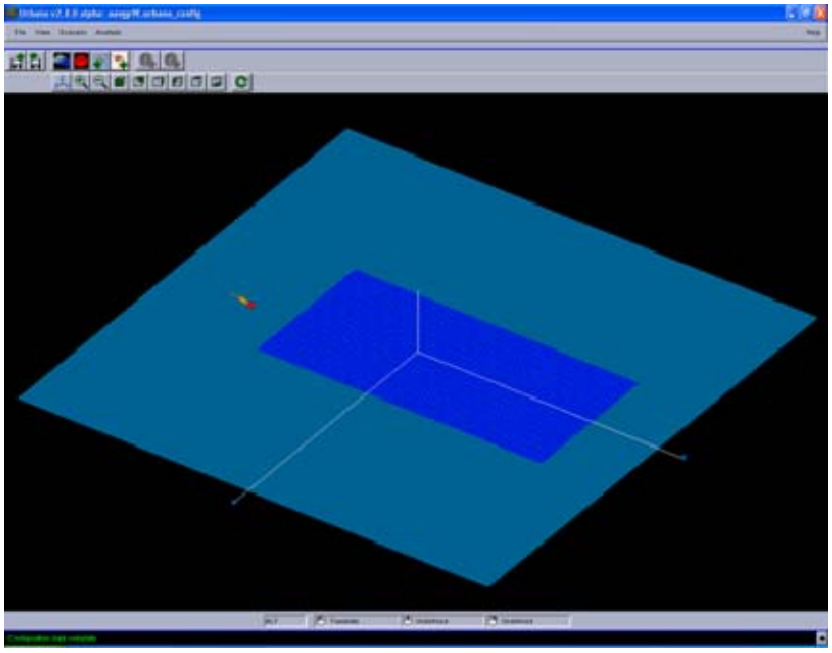

Figure 21. UAV position one.

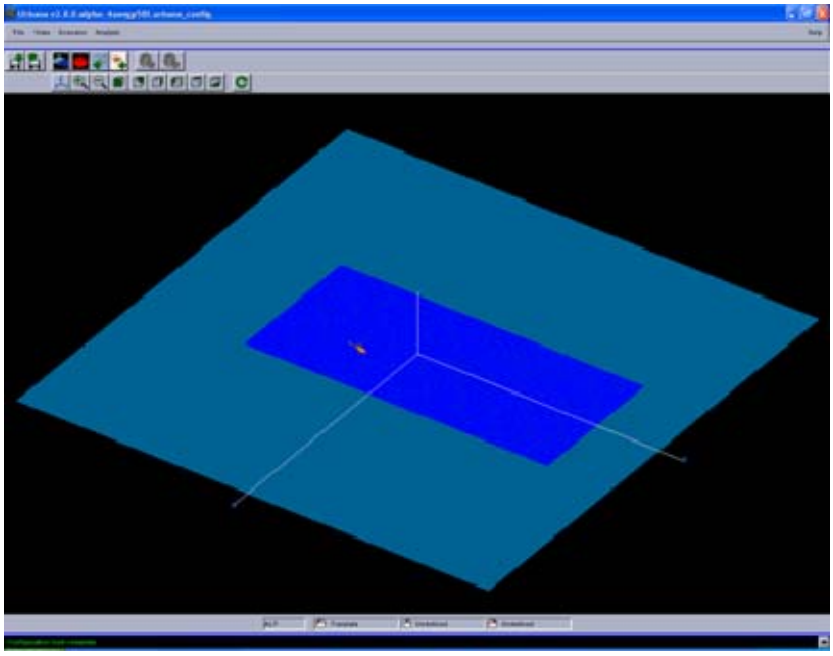

Figure 22. UAV position two.

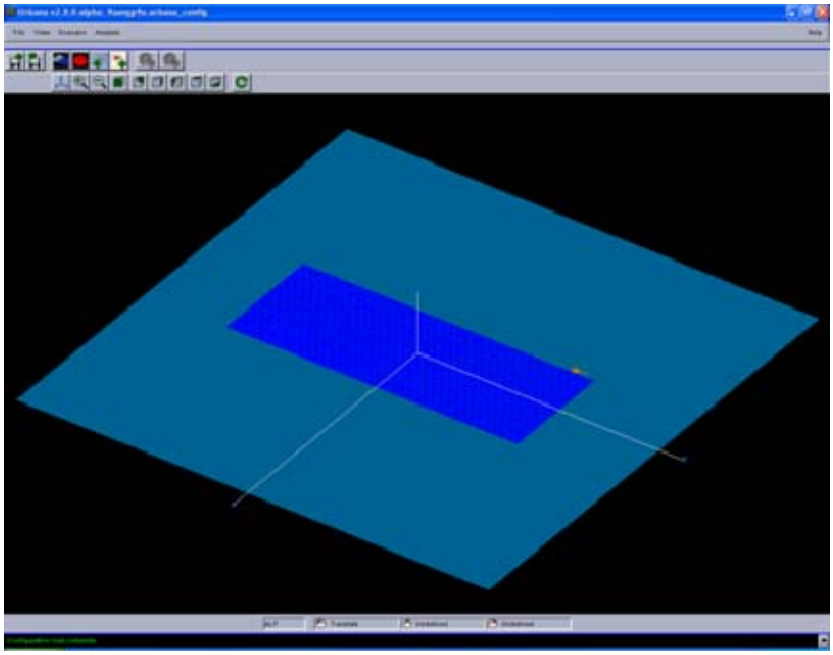

Figure 23. UAV position three.

5. Observation Points

The observation points can be specified interactively in *iUrbana* or in a file. The observation region is limited to the ship deck in most cases, because that is where the operator would most likely be located.

6. Analysis Parameters

Geometrical optics improves on the free-space by using shooting-and-bouncing rays (SBRs) and edge diffraction to evaluate fields on the observation surface. To compare the results, all the simulations are run both with and without the diffraction option. The number of rays and number of bounces calculated are specified in the methods panel after selecting Geometric Optics.

The Ray Burst Interval text box in the **Analysis** slot specifies the degree angle between the rays when shot from the antenna. The lower this value is, the greater the accuracy of the results but the greater the runtime. The recommended value is 2 degrees. Anything above 5 degrees may result in inaccurate results. Anything less than 1 degree will result in a large amount of computation time.

The Maximum Number of Ray Bounces controls the number of bounces that the program will compute before moving to the next ray shot. The greater this value, the greater the accuracy of the results will be, at the cost of runtime. The *Urbana* engine will automatically stop tracing rays that have been absorbed regardless of this value.

Single Diffraction is used in some of the scenarios. To use this function, it is necessary to use an **.edge* file.

To transform an **.facet* file to a **.edge* file a *Menelaus* command was used with following form: *menelaus −mkedge file.facet file.edge -120*.

7. Frequencies

The standard wireless frequencies were used (ISM band). For the current research simulating data links over a Navy Ship, center frequencies of 900 MHz, 2.4 GHz, and 5 GHz are selected.

8. UAV with Ground Plane Simulations

The initial step was to determine the transmission results for the antenna from the UAV without the DDG Frigate Ship, and analyze the difference between the antenna with vertical polarization and horizontal polarization. The *Urbana* software provides two types

of outputs: an ASCII file and a contour plot. Figures 24-26 show the contour plot at the three UAV positions. The results of the vertical polarization for the first position of the UAV are shown in the Figure 24. The values used are summarized in Table 4.

Input Parameters	Values
iUrbana file	*uavgroundplane6900.urbana_config*
Facet File	*gpuav1.facet*
Edge File	None
Observation plane file	None
Antenna type	*test.antpat*
Antenna power (W)	1
Antenna polarization	Vertical
Antenna frequency	900 MHz
Antenna coordinates (x,y,z)	*x*= 34m, *y*= -49m, *z*= 21m (in meters)
Propagation mechanism	GO
Edge diffraction	NO
Ray angular intervals	2
Max ray bounces	10
Coating materials	PEC
Power	30 dBm

Table 4. Input parameters for Figure 24.

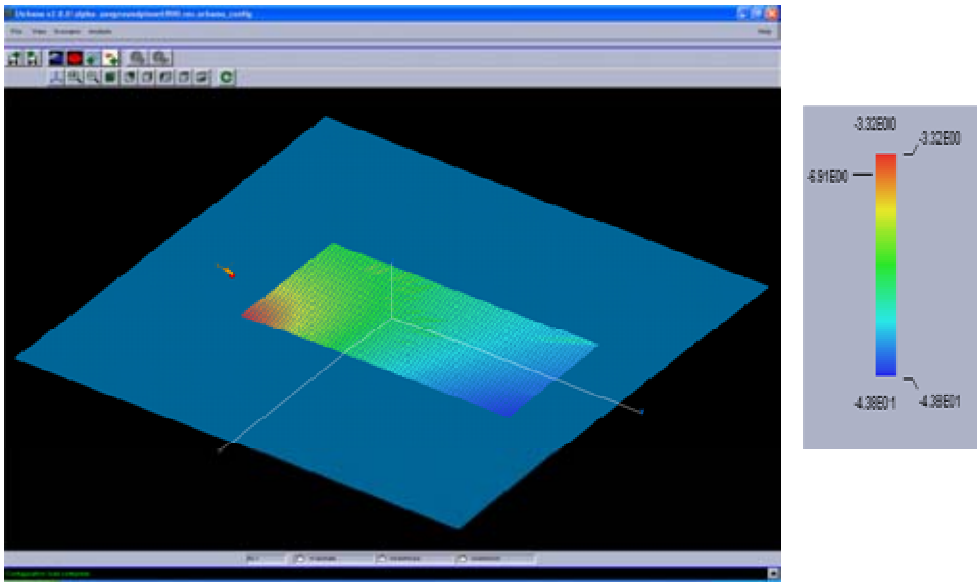

Figure 24. Signal distribution for UAV position one, vertical polarization, for the data in Table 4, the values of the field are in dB V/m.

The same antenna pattern file was used with the three different frequencies, so the results are the same. Only the results of the 900 MHz frequency are shown.

It is clear that the biggest power is concentrated in the corner of the coverage region, which has a size of 120.05 m by 58.62 m. The signal values go from -43.81 dB V/m to -3.3193 dB V/m.

The results of the horizontal polarized antenna are presented in Figure 25. The input values used are summarized in Table 5.

Input Parameters	Values
iUrbana file	*uavgroundplane8900.urbana_config*
Facet File	*gpuav1.facet*
Edge File	None
Observation plane file	None
Antenna type	*test.antpat*
Antenna power (W)	1
Antenna polarization	Horizontal
Antenna frequency	900 MHz
Antenna coordinates (x,y,z)	*x*= 34m, *y*= -49m, *z*= 21m (in meters)
Propagation mechanism	GO
Edge diffraction	NO
Ray angular intervals	2
Max ray bounces	10
Coating materials	PEC

Table 5. Input parameters for Figure 25.

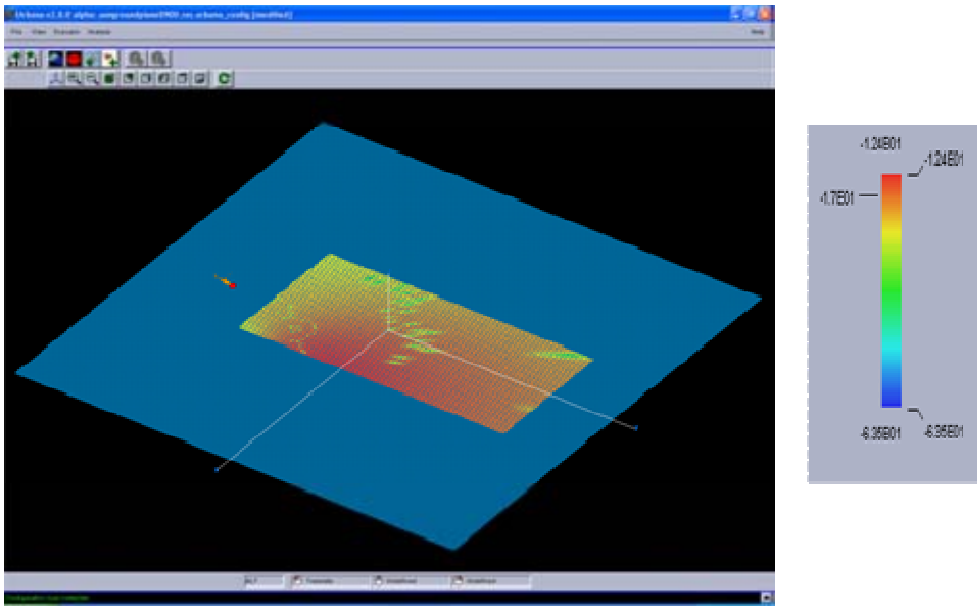

Figure 25. Results for forward looking antenna without the DDG Frigate Ship, UAV position one, for the input in Table 5, the values of the field are in dB V/m.

The values of the power received are at the maximum values in all the coverage areas with just a little zone of smaller values. The values go from -63.52 dB V/m to -12.42 dB V/m.

B. TRANSMISSION BETWEEN UAV AND DDG FRIGATE SHIP

To complete the experiment to analyze the effect of the structure present on the main deck of a ship in transmission of electromagnetic signals, 36 different scenarios were run in *Urbana*, using three different positions of a flight pattern of the UAV over the DDG ship. The positions are mentioned in Table 3.

Three frequencies, 900 MHz, 2.4 GHz and 5.8 GHz were used. Also two polarizations, vertical and horizontal, and geometric optics was used with single diffraction and without it.

The file *ddgpoints.obv* that contains 564 squares localized on the main deck of the *DDG.facet* file was created with *Matlab.* This file can be used as the input of the file *read_field_file.m*, shown in Appendix B, to get the values of the power received over the main deck. The sample result of this program is shown in Figure 26.

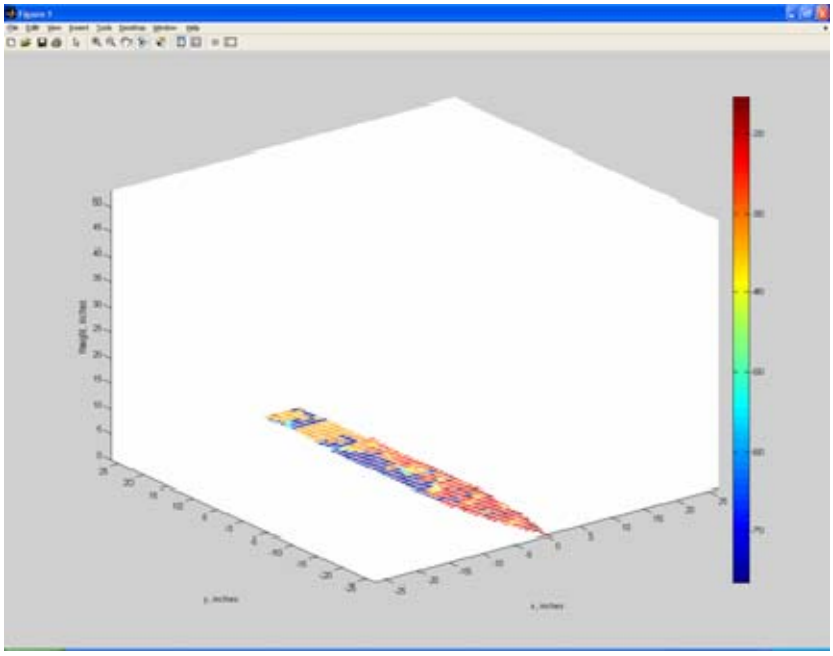

Figure 26. Illustrative result of power received with *read_field_file.m.* The values of the field are in dB V/m.

Urbana also shows the results in its GUI, as is shown in Figure 27. The location of the coverage region is superimposed over the *DDG.facet* file.

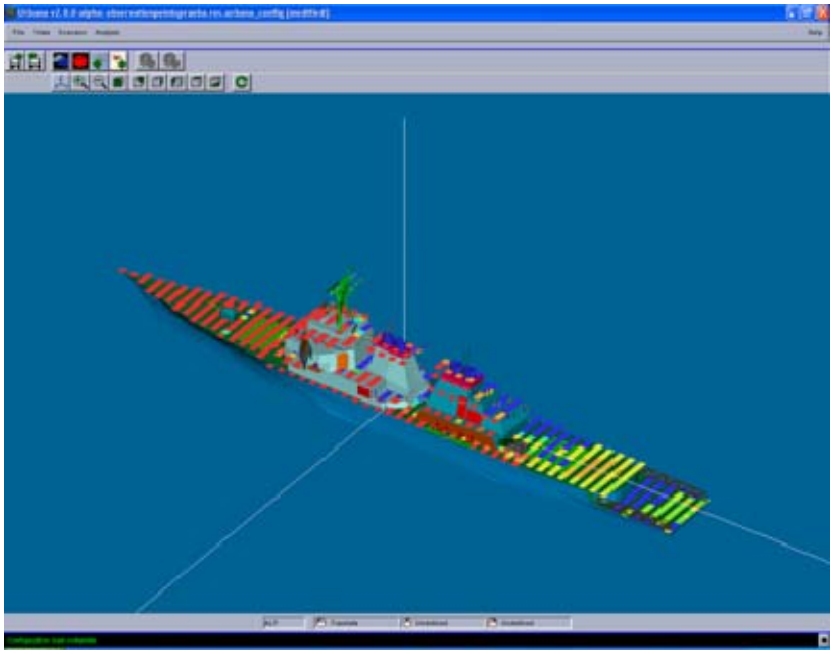

Figure 27. Illustrative result showing the *DDG.obv* file used to create a coverage region for the simulation.

Each square's location is determined by using values for x, y and z, such that all the squares are on the surface. Only the most relevant image results are presented here.

First is a comparison between the scenarios with the same frequency 2.4 GHz and 1 Watt power, but changing only the use of diffraction. In all the cases, graphically it is clear to see that the use of the single diffraction gives the best power reception.

An undesirable characteristic of the results generated without diffraction is the presence of a shadow on the opposite side of the antenna illumination, as shown in Figure 28(a). Diffraction provides a means of propagation into shadows.

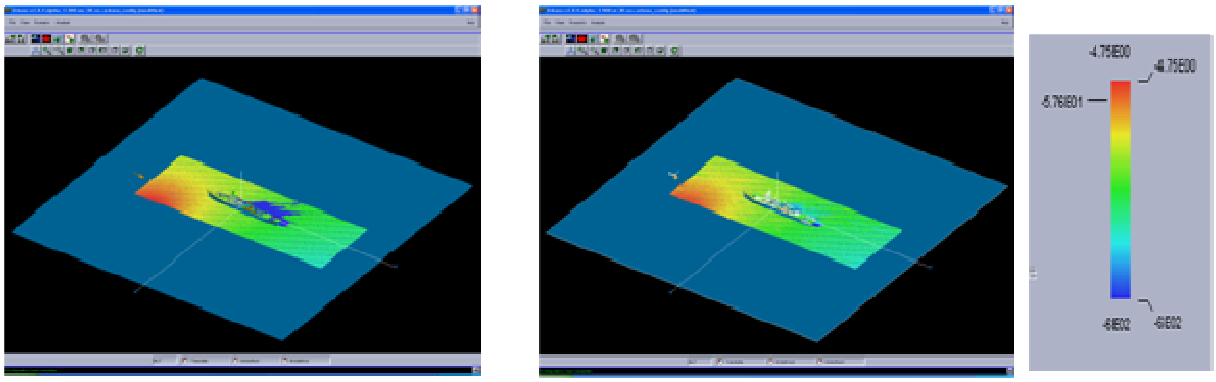

(a) Without diffraction (b) With diffraction

Figure 28. Comparison of the use of single diffraction and without it, the values of the field are in dB V/m.

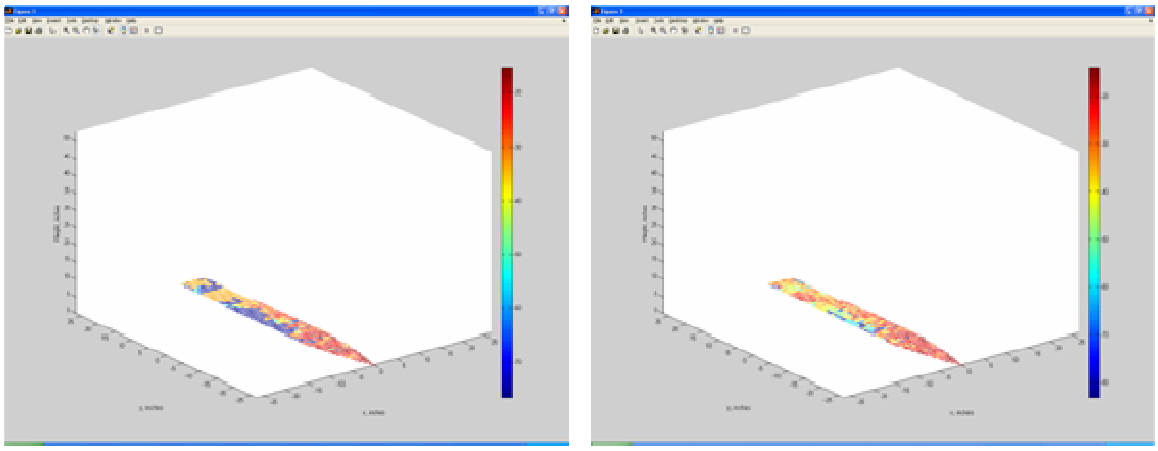

(a) Without diffraction (b) With diffraction

Figure 29. *Matlab* results for Figure 28, the values of the field are in dB V/m.

In Figure 29 the results from *Matlab* are shown for the data in Figure 28. In Figure 28(a), the starboard side at the midship is completely blocked by the bridge and the structures located at midship, showing a blue color that represents values less than -60 dB V/m. In Figure 28 (b), using single diffraction, the blue area is smaller and only two or three squares show the lowest value and the red area that represents -13 to -14 dB V/m covers 70% of the main deck.

In other comparisons, the polarization of the antenna and the position of the UAV produce different values of the power reception on the ground plane and the ship. The results in Figures 30 and 31 show that using vertical polarization for this UAV position only permits very good reception in the corner near the UAV. On the other hand, using the horizontal polarization, there is very good reception in almost all the coverage region, where the minimum value is -60 dB V/m and the maximum value is -0.9 dB V/m. Figure 31 shows the *Matlab* results for Figure 30.

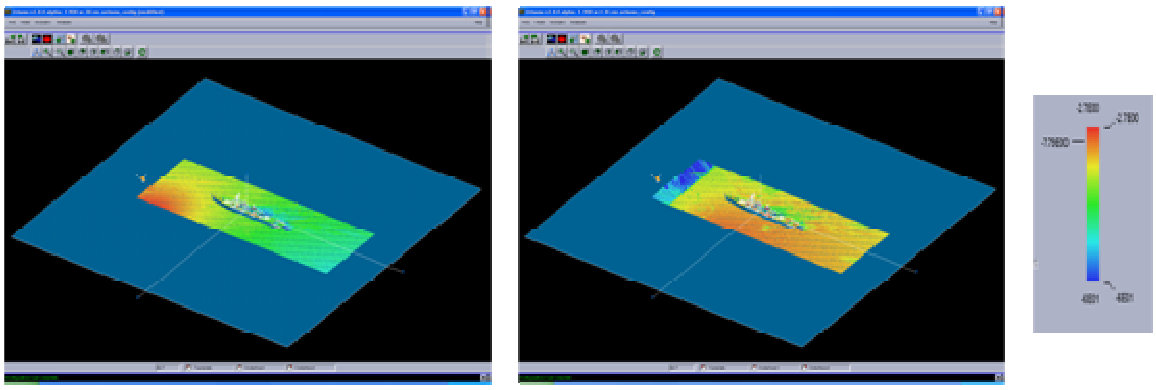

(a) Without diffraction (b) With diffraction

Figure 30. Comparison of vertical and horizontal polarization at the same frequency, the values of the field are in dB V/m.

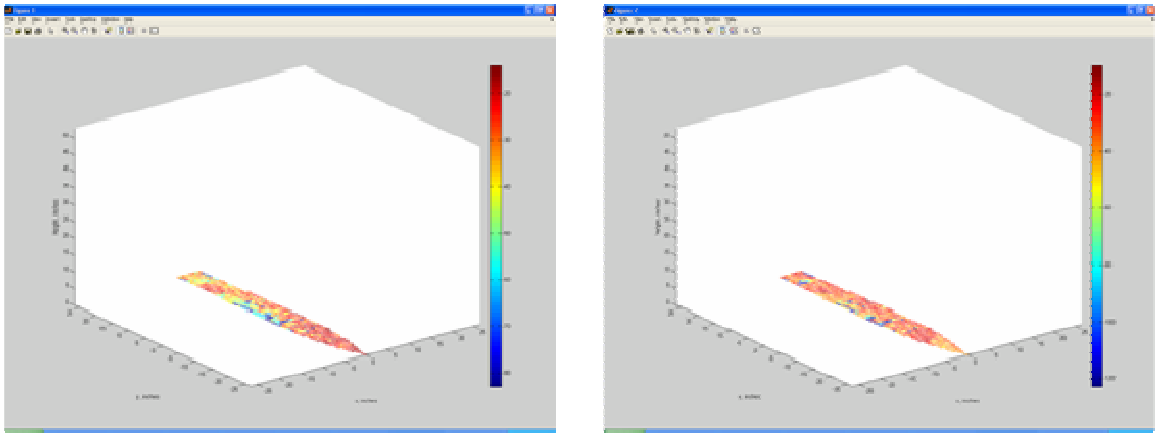

(a) Without diffraction (b) With diffraction

Figure 31. *Matlab* results for Figure 30, the values of the field are in dB V/m.

Figures 32, 33 and 34 show the difference between the three frequencies, 900 MHz, 2400 MHz and 5800 MHz, using single diffraction and the antenna with horizontal polarization.

The best reception of all is with 5800 MHz, while 2400 MHz is better than 900 MHz. Therefore the conclusion is that the higher the frequency the better the reception. *Matlab* results are shown in Figures 35, 36 and 37, respectively.

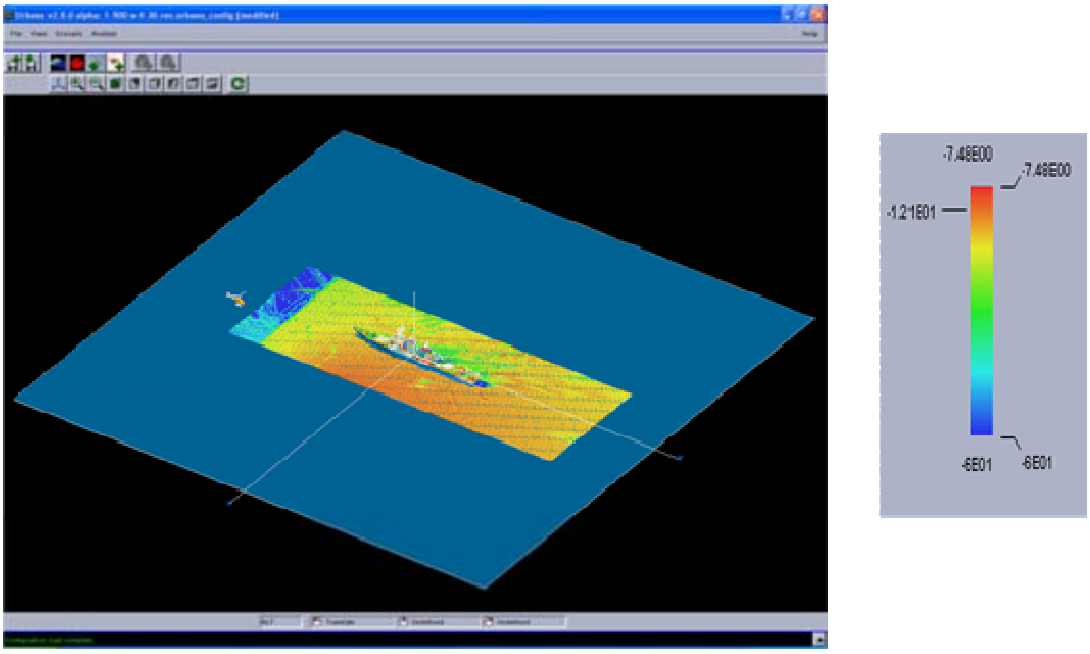

Figure 32. Frequency: 900 MHz, UAV position one, the values of the field are in dB V/m.

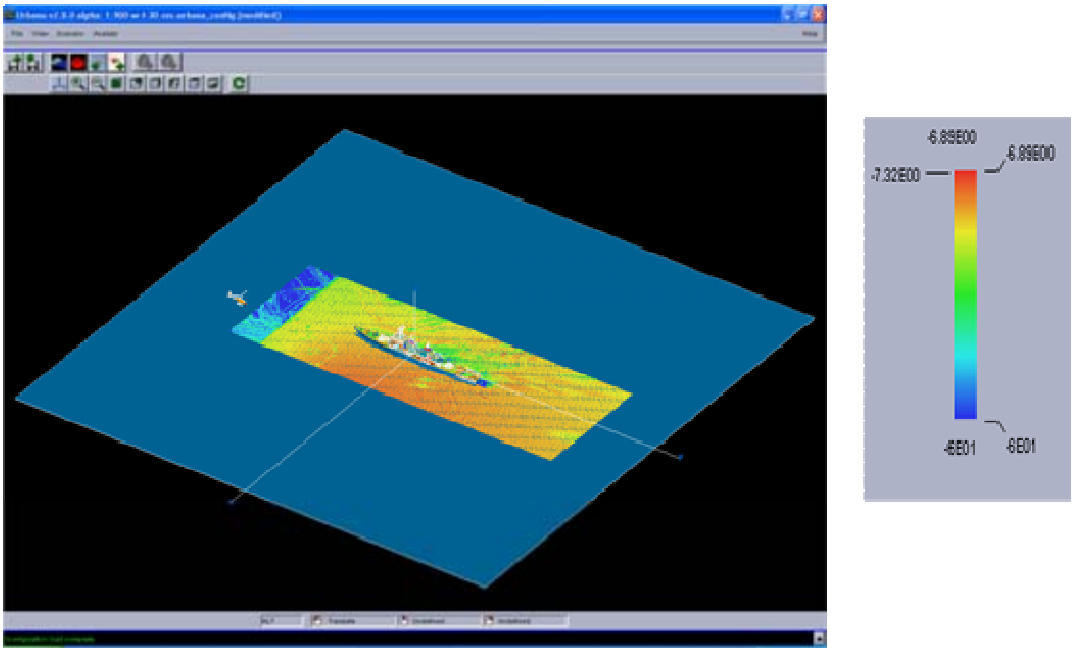

Figure 33. Frequency: 2400 GHz, UAV position 1, the values of the field are in dB V/m.

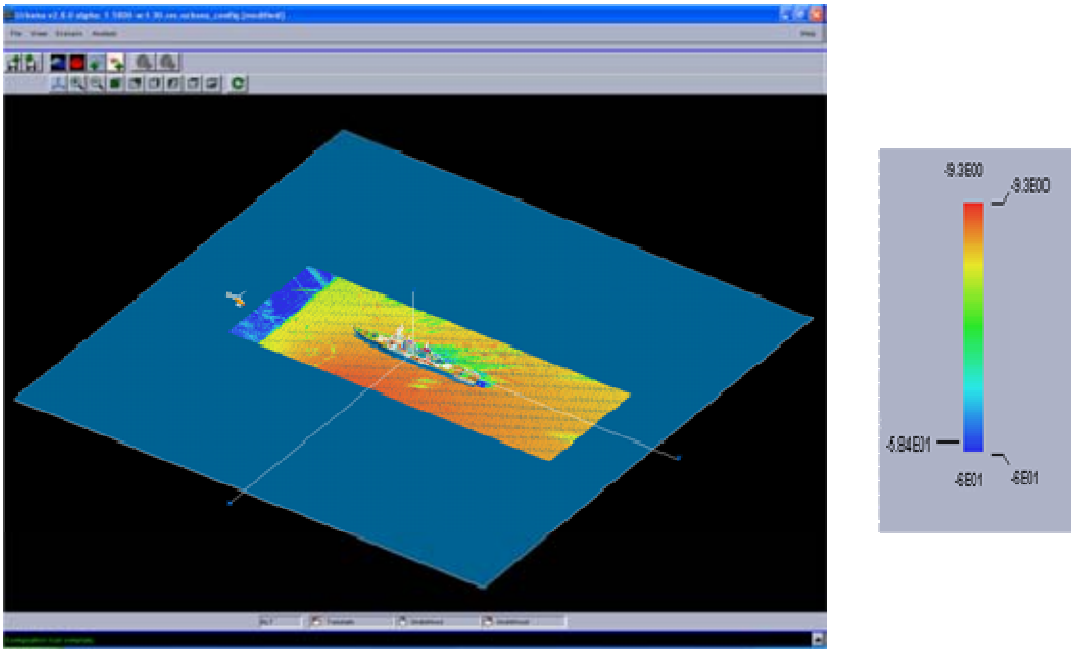

Figure 34. Frequency: 5800 GHz, UAV position 1, the values of the field are in dB V/m.

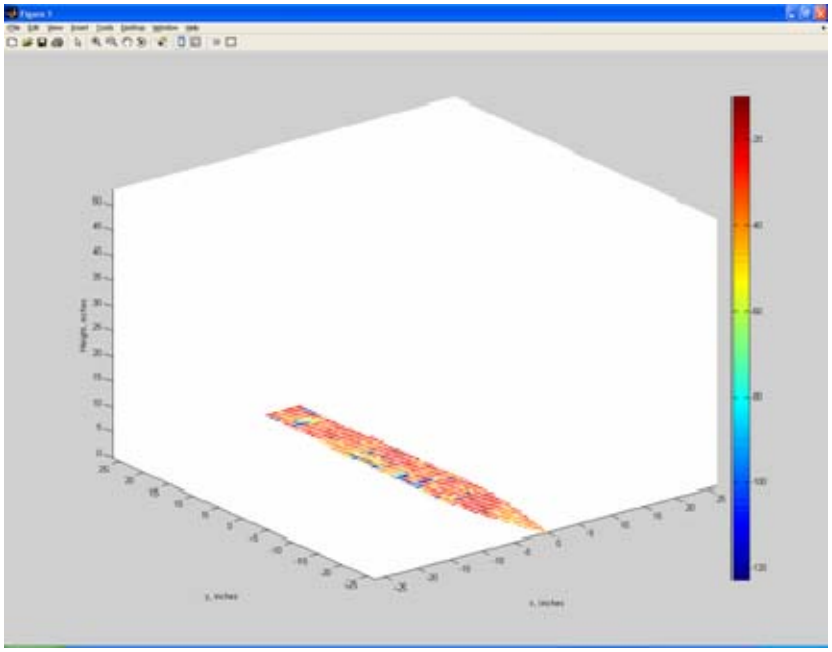

Figure 35. *Matlab* results for Figure 32, frequency: 900 MHz.

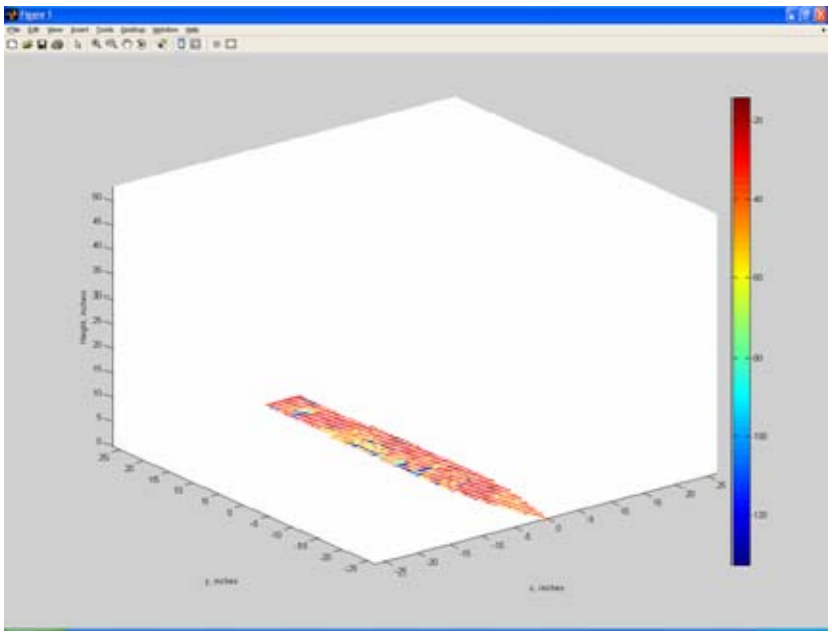

Figure 36. *Matlab* results for Figure 33, frequency: 2400 MHz.

Figure 37.

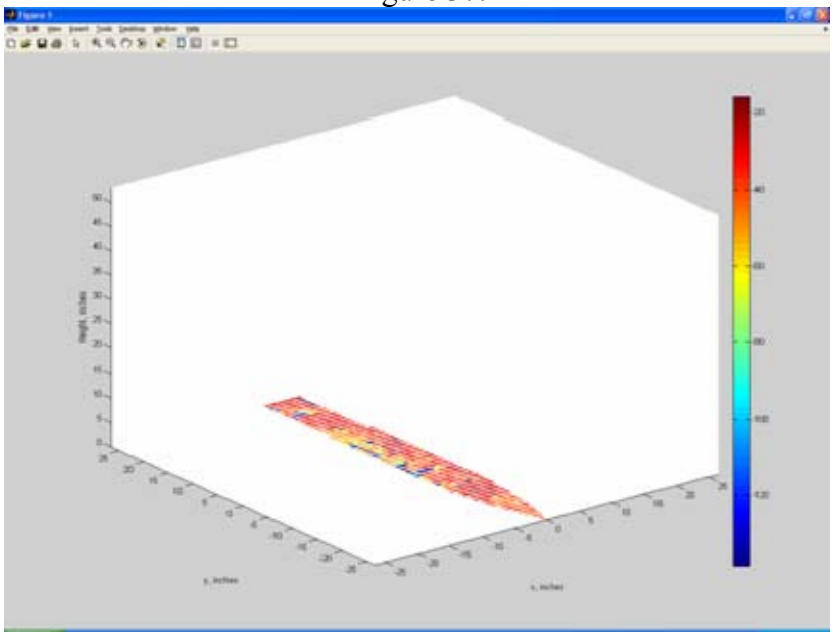

Figure 38. *Matlab* results for Figure 34, frequency: 5800 MHz.

Figures 38 and 40 present the results of the scenarios summarized in Tables 6 and 7. For position two, the best result is presented in Figures 38 and 40. The coverage of the antenna with vertical polarization is complete, but Figure 41 shows that the coverage of the antenna with horizontal polarization is only present in the middle of the observation region.

Input Parameters	Values
Input value	*4-900-w-30.urbana_config*
Facet File	*gpuav4.facet*
Edge File	*gpuav4.edge*
Observation plane file	None
Antenna type	*test.antpat*
Antenna power (W)	1
Antenna polarization	Vertical
Antenna frequency	900 MHz
Antenna coordinates (x,y,z)	*x*= 34m, *y*= -49m, *z*= 21m (in meters)
Propagation mechanism	GO
Edge diffraction	NO
Ray angular intervals	2
Max ray bounces	10
Coating materials	PEC

Table 6. Input parameters for Figure 38.

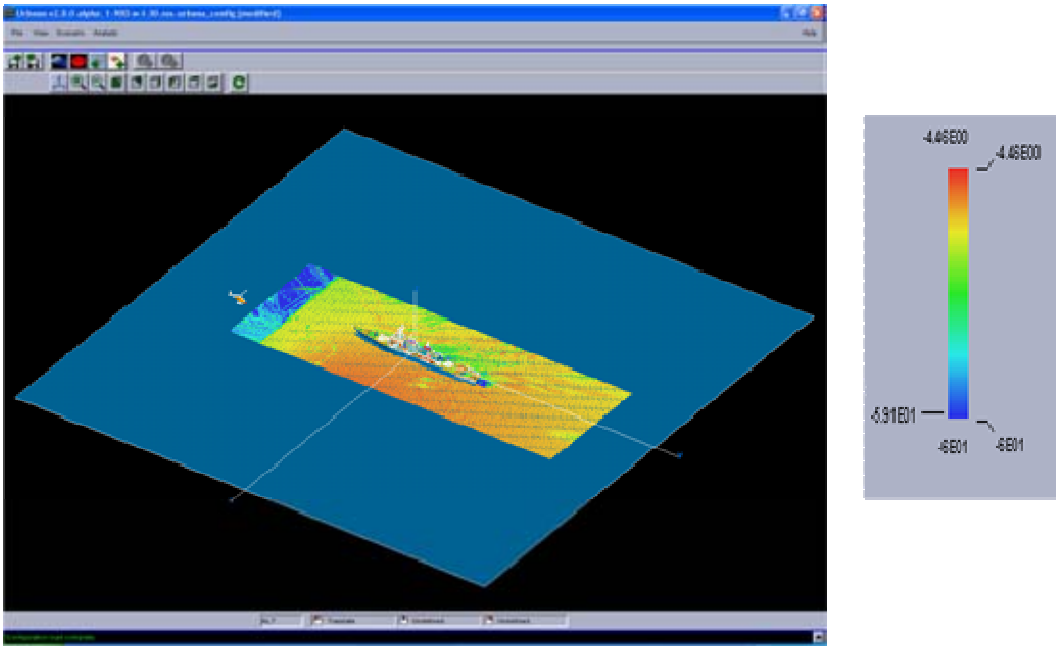

Figure 39. Position two, frequency: 900 MHz, vertical polarization. The values of the field are in dB V/m.

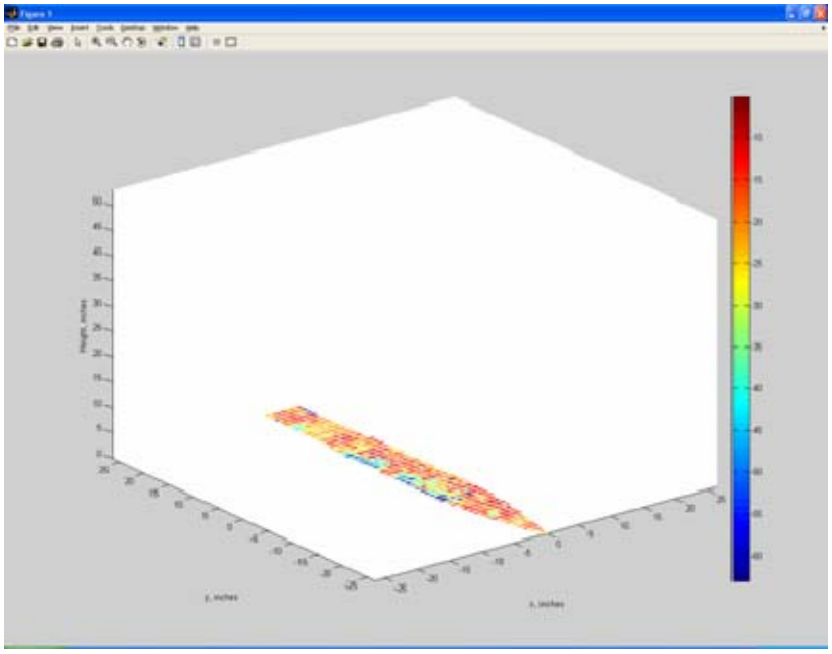

Figure 40. *Matlab* results for Figure 38.

Input Parameters	Values
Input value	*4-900-w-f-30.urbana_config*
Facet File	*gpuav4.facet*
Edge File	*gpuav4.edge*
Observation plane file	None
Antenna type	*test.antpat*
Antenna power (W)	1
Antenna polarization	Horizontal
Antenna frequency	900 MHz
Antenna coordinates (x,y,z)	*x*= 34m, *y*= -49m, *z*= 21m (in meters)
Propagation mechanism	GO
Edge diffraction	NO
Ray angular intervals	2
Max ray bounces	10
Coating materials	PEC

Table 7. Input parameters for Figure 40.

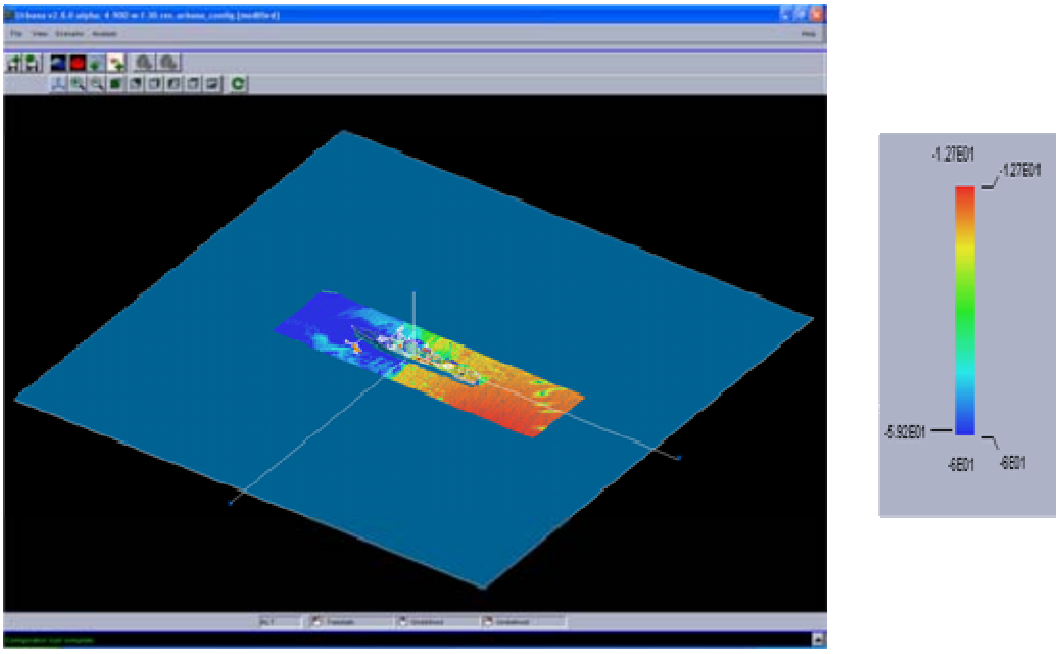

Figure 41. Position two, frequency: 900 MHz, vertical polarization. The values of the field are in dB V/m.

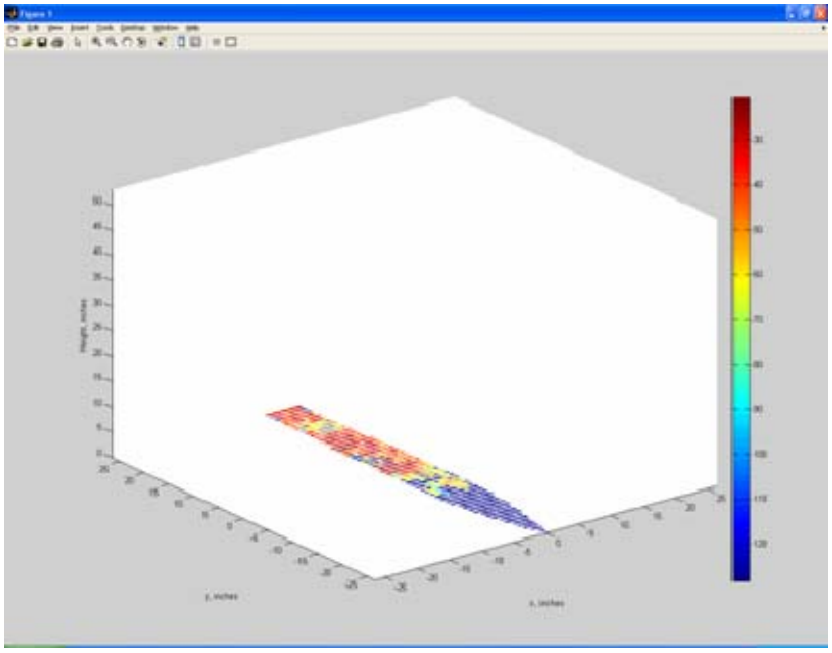

Figure 42. *Matlab* results for Figure 40.

The comparison between the three different frequencies that use horizontal polarization does not present any special difference between them, but in all cases only about half of the coverage area has reception of signal.

Input Parameters	Values
Input value	*9-900-w-f.urbana_config*
Facet File	*gpuav4.facet*
Edge File	*gpuav4.edge*
Observation plane file	None
Antenna type	*test.antpat*
Antenna power (W)	1
Antenna polarization	Vertical
Antenna frequency	900 MHz
Antenna coordinates (x,y,z)	*x*= 34m, *y*= -49m, *z*= 21m (in meters)
Propagation mechanism	GO
Edge diffraction	NO
Ray angular intervals	2
Max ray bounces	10
Coating materials	PEC

Table 8. Input parameters for Figure 45.

In the analysis of the UAV transmitting from position three it is clear that in the area near the UAV there is a very high reception with the antenna, as shown in Figures 42 and 43.

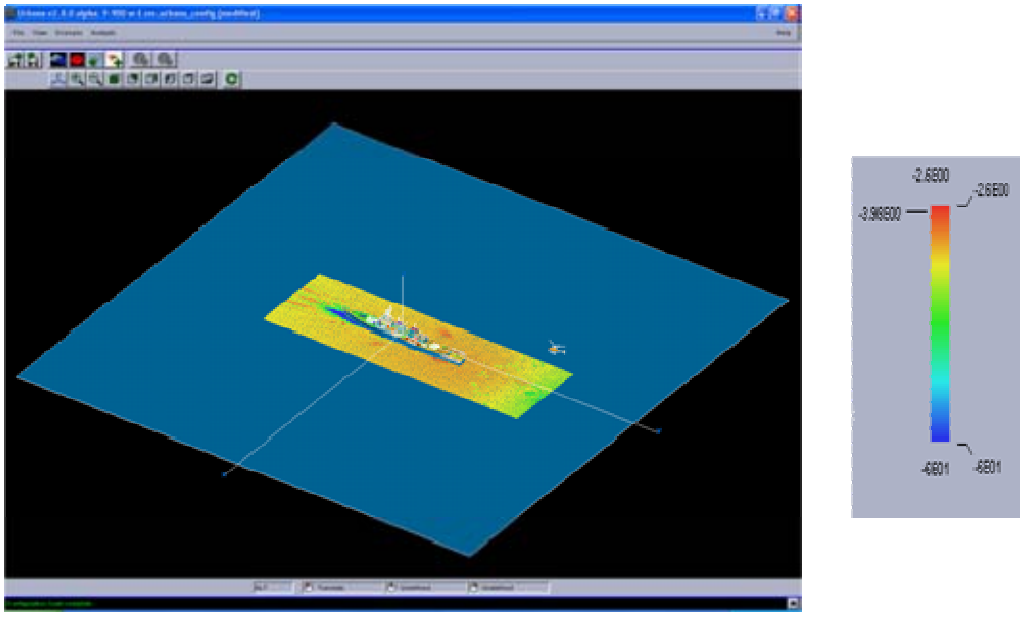

Figure 43. Position three, Frequency: 900 MHz, horizontal polarization. The values of the field density are in dB V/m.

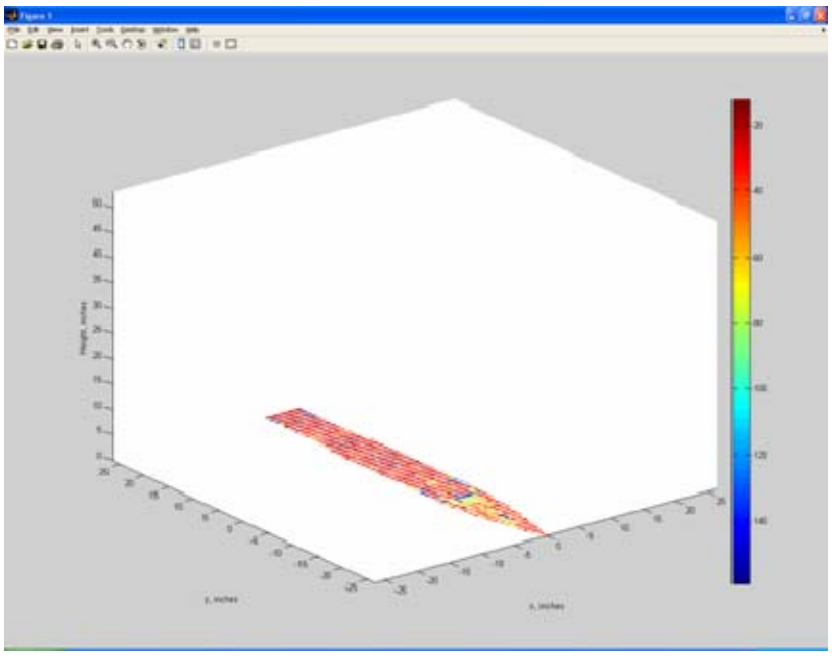

Figure 44. *Matlab* results for Figure 42.

C. CARGO SHIP SIGNAL COVERAGE

Another important problem is the ability to communicate from interior ship spaces to the upper deck. If there are not a sufficient number of openings for signals to penetrate, then coverage on the deck will be limited.

One possible solution is to use relay antennas that pick up signals inside and then transmit by wire through the bulkheads and retransmit from a second antenna mounted outside. A series of simulations was performed with a cargo ship model to assess several antenna locations.

The objective is to find the best place to locate an antenna to transmit so as to have reception on all the main deck. Four different positions were examined for the antenna. The coordinates for each one are summarized below in Table 9.

POSITION	X	Y	Z
POSITION ONE	**-5**	**62**	**21.7**
POSITION TWO	**-5.5**	**60**	**21.7**
POSITION THREE	**-5**	**102**	**20**
POSITION FOUR	**-5**	**65**	**44**

Table 9. Antenna positions for the cargo ship problem.

In position one the antenna is located inside the bridge as shown in Figure 44. Only the front part of the ship received the signal emitted by the antenna, because the windows in the bridge are made with glass material. The energy mainly passes through the large bridge observation windows (on the left wall in Figure 19.) The *Matlab* results are shown in Figure 45.

Input Parameters	Values
Input value	*Cargoship_ref.res.urbana_config*
Facet File	*cargom2.facet*
Edge File	*cargom3.edge*
Observation plane file	None
Antenna type	*shdip.antpat*
Antenna power (W)	1
Antenna polarization	Vertical
Antenna frequency	2.4 GHz
Antenna coordinates (x,y,z)	*x*= -5m, *y*= 62m, *z*= 21.7m
Propagation mechanism	GO
Edge diffraction	YES
Ray angular intervals	2
Max ray bounces	10
Coating materials	PEC, and glass.

Table 10. Input parameters for Figure 44.

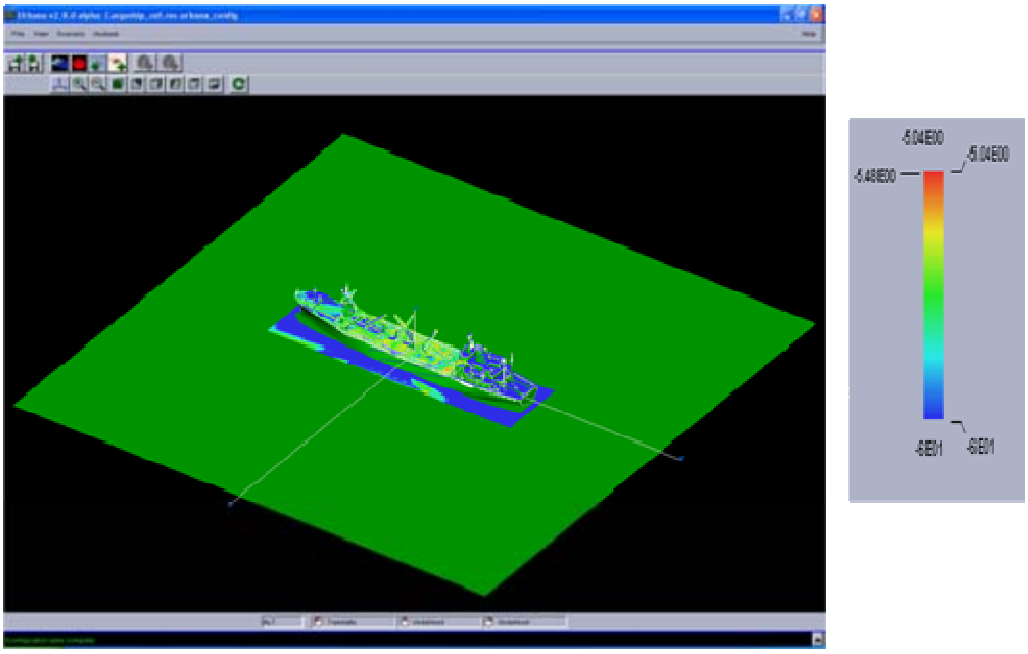

Figure 45. Antenna located inside the bridge. The values of the field are in dB V/m.

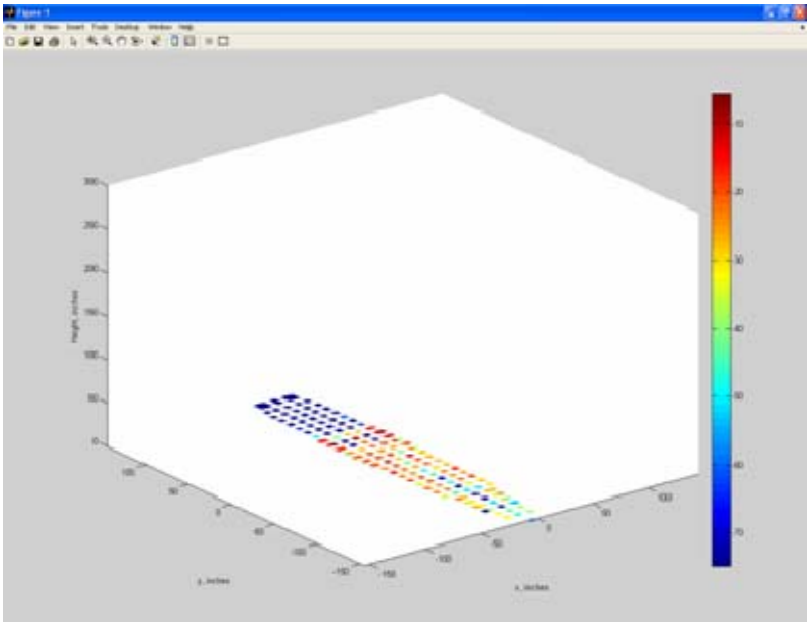

Figure 46. *Matlab* results for Figure 44.

With the antenna outside the bridge, 90% of the main deck and the front of the bridge show a power received with values between -35 dB V/m and -45 dB V/m, and the areas near the cranes and masts in the main deck present a very low reception (on the order of -60 dB V/m). The results are shown in Figures 46 and 47.

Input Parameters	Values
Input value	*Cargoship_outsidenr_.res.urbana_config*
Facet File	*cargom2.facet*
Edge File	*cargom3.edge*
Observation plane file	None
Antenna type	*shdip.antpat*
Antenna power (W)	1
Antenna polarization	Vertical
Antenna frequency	2.4 GHz
Antenna coordinates (x,y,z)	*x*= -5.5m, *y*= 60m, *z*= 21.7m
Propagation mechanism	GO
Edge diffraction	YES
Ray angular intervals	2
Max ray bounces	10
Coating materials	PEC, and glass.

Table 11. Input parameters for Figure 46.

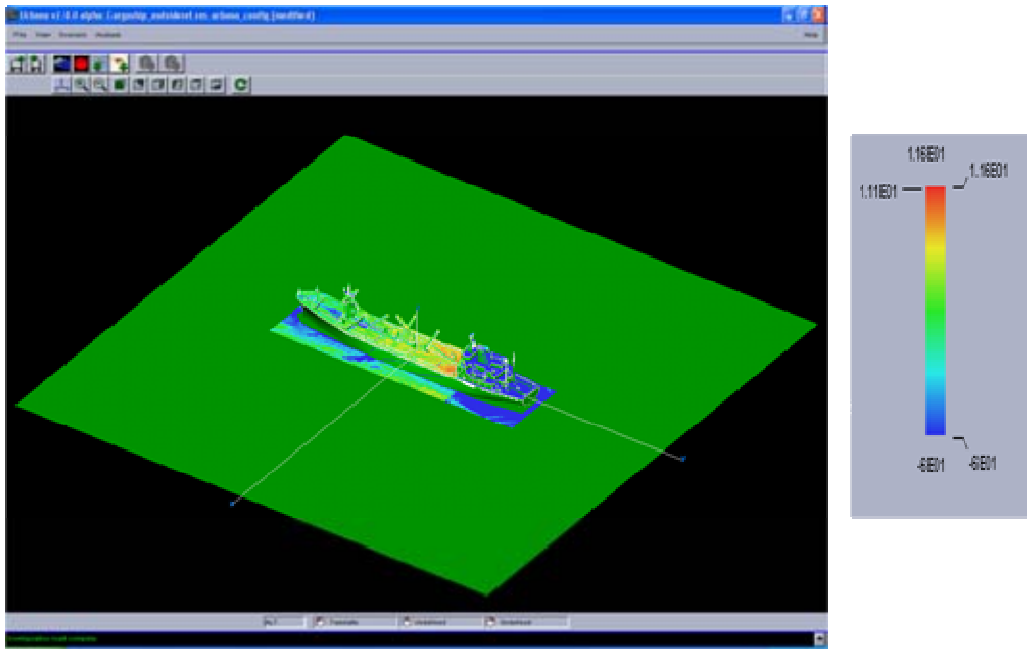

Figure 47. Antenna located in front of the bridge (Table 11). The values of the field are in dB V/m.

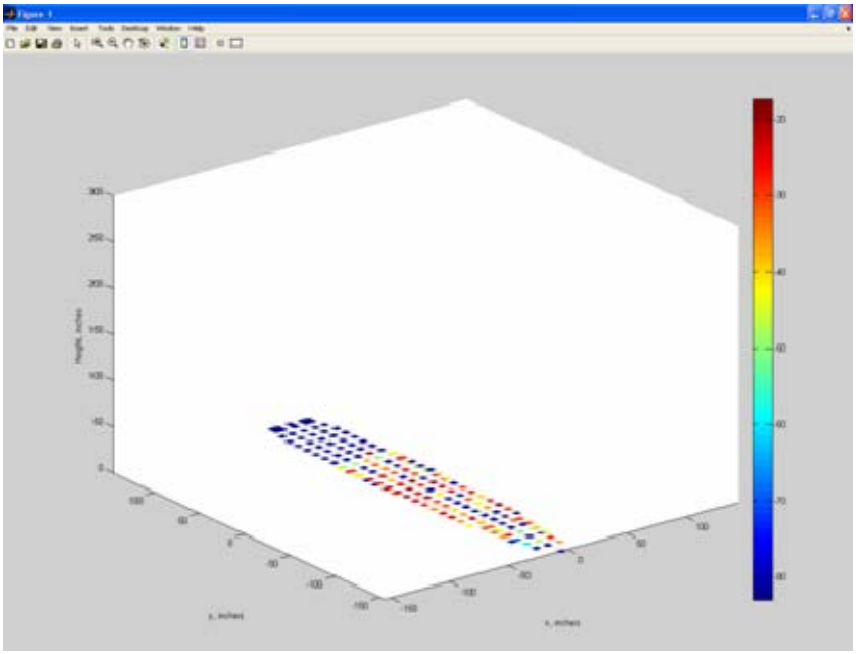

Figure 48. *Matlab* results for Figure 46.

In the scenario in Figure 46, the antenna is located just 0.5 meters in front of the bridge. It is now outside of the deck house and the difference in the results is notable. The area near the bridge has values of -16.6 dB V/m.

Input Parameters	Values
Input value	*Cargoship_sternref.res.urbana_config*
Facet File	*cargom2.facet*
Edge File	*cargom3.edge*
Observation plane file	None
Antenna type	*shdip.antpat*
Antenna power (W)	1
Antenna polarization	Vertical
Antenna frequency	2.4 GHz
Antenna coordinates (x,y,z)	*x*= -5m, *y*= 102m, *z*= 20m
Propagation mechanism	GO
Edge diffraction	YES
Ray angular intervals	2
Max ray bounces	10
Coating materials	PEC, and glass.

Table 12. Input parameters for Figure 48.

In the scenario in Figures 48 and 49, the antenna is located in the back part of the bridge, to see its effect on the values of the reception in the stern of the ship. The signal cannot reach any area of the front part of the ship because the structure of the bridge does not permit propagation of the signal.

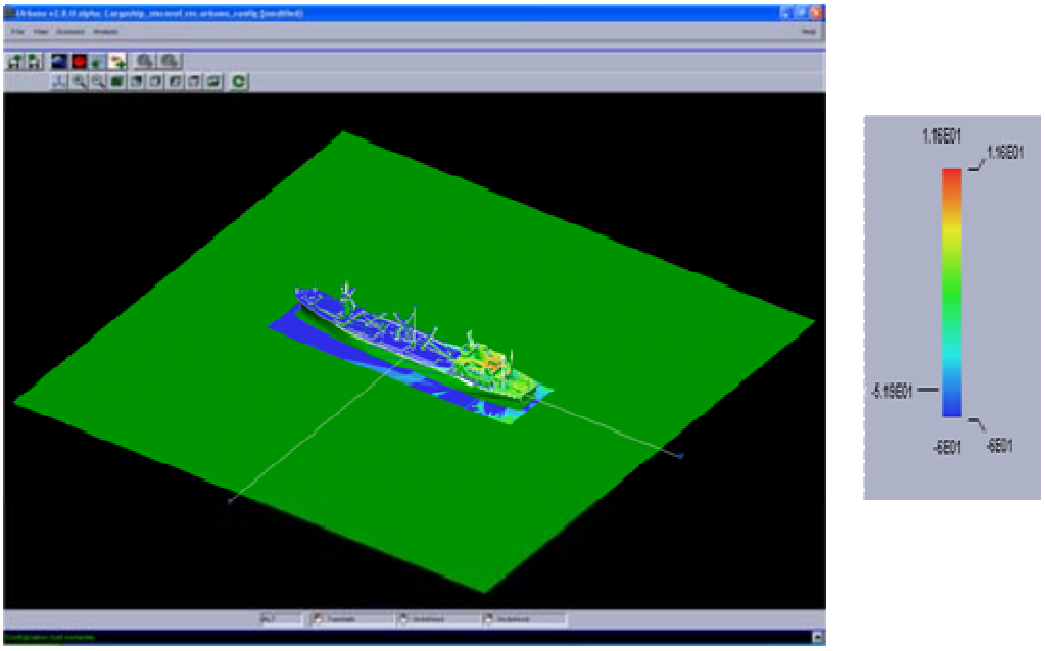

Figure 49. Antenna located on the back of the bridge (Table 12). The values of the field are in dB V/m.

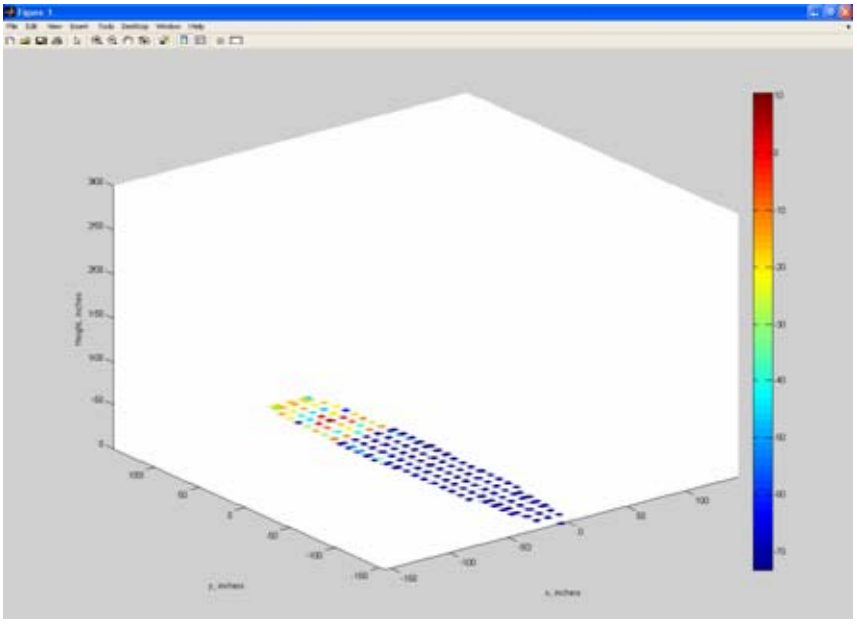

Figure 50. *Matlab* results for Figure 48.

Input Parameters	Values
Input value	*Cargoship_upref.res.urbana_config*
Facet File	*cargom2.facet*
Edge File	*cargom3.edge*
Observation plane file	None
Antenna type	*shdip.antpat*
Antenna power (W)	1
Antenna polarization	Vertical
Antenna frequency	2.4 GHz
Antenna coordinates (x,y,z)	*x*= -5m, *y*= 65m, *z*= 44m
Propagation mechanism	GO
Edge diffraction	YES
Ray angular intervals	2
Max ray bounces	10
Coating materials	PEC, and glass.

Table 13. Input parameters for Figure 50.

Finally, the antenna is located on the upper part of the mast at 44 meters above the main deck (Figure 50). In this position all the area of the main deck has reception with values between -30 dB V/m to -40 dB V/m. In this scenario the one superstructure in the astern does not permit propagation in some areas, but these are areas that are not in the normal maneuvering of the ship, and are not important.

The minimum field value of this exercise is -60 dB V/m and the maximum value is -12.41 dB V/m.

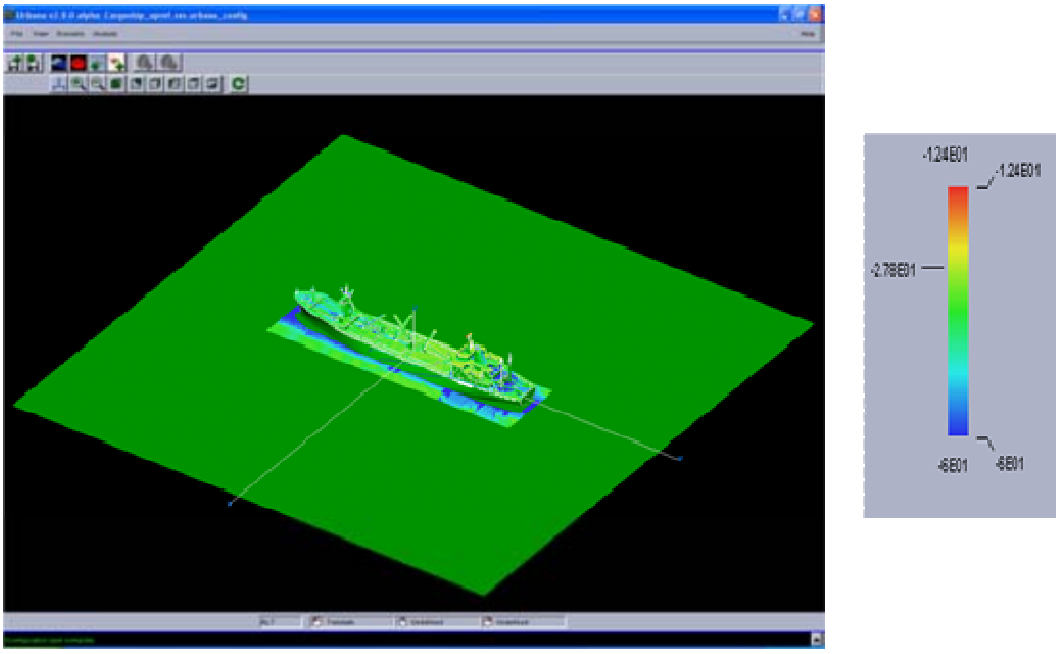

Figure 51. Antenna located in the mast. (Table 13). The values of the field are in dB V/m.

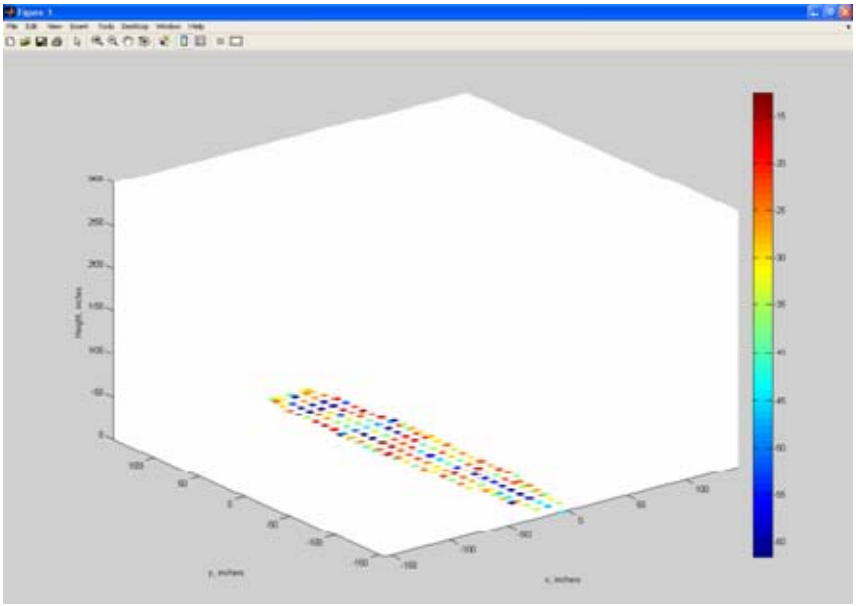

Figure 52. *Matlab* results for Figure 50.

THIS PAGE INTENTIONALLY LEFT BLANK

V. CONCLUSIONS AND RECOMMENDATIONS

A. CONCLUSIONS

The primary objective of this thesis was to investigate the propagation of wireless signals on the main deck of a ship and the effect of the structures in different shipboard environments.

Two different scenarios were selected. In the first situation a UAV transmits to a DDG Frigate Ship. This topic is a very important situation because nowadays the proliferation of UAVs has begun to present some problems with jamming and interference by friendly forces.

The second scenario presents an antenna installed onboard a cargo ship at different positions, trying to find the best relay antenna position to get coverage on all the areas of the main deck.

The *Urbana* software package was used as the simulation tool. The frequencies 900 MHz, 2.4 GHz and 5.8 GHz were selected because most of the wireless systems operate at frequencies above 900 MHz.

In Chapter IV, some examples were developed to assess the performance of the *Urbana* code and validate its use in complex and challenging propagation environments. In all the scenarios geometrical optics was used. Three positions in the flying pattern of the UAV, and both vertical and horizontal polarization were used. Single diffraction was used in half of the situations to get a best idea of the different results in this situation. Then an analysis of the outcomes for different input parameters to the *Urbana* input file was conducted.

The results show that using a higher frequency generally yields better reception onboard. Overall there is no advantage of one polarization over the other.

In the cargo ship scenario, is necessary to find a position of the relay antenna outside of the bridge, and in a very high position to reach all the areas of the main deck. There will always be spaces with very poor reception, but they can be limited to ones that

are not directly related to the areas in which the crew need good reception to conduct the normal operations onboard a ship of this type.

Urbana is a good tool to give very detailed information of the results of special electromagnetic systems and environments, and allows for the modification of all the parameters of a scenario.

Also, the simulations in *Urbana* permit the Navy to save money, because it is not necessary to perform an experiment in real life using the ship, the vehicle and all the people that an experiment of this magnitude involves.

B. FUTURE WORK

Future work might include the investigation of new models of combat ships in the U.S. Navy such as the Littoral Combat Ship (LCS) and the new role and functions of this ship in Naval operations.

Also, it is important to analyze and study a scenario of two UAVs, or a UAV and another kind of military airplane, to analyze the effects of electromagnetic transmissions and interference.

APPENDIX

This Appendix includes two *Matlab* codes, one to create an antenna pattern to be used in *Urbana*, and the other used to read the field file created in *Urbana*.

A. ANTENNA PATTERN FILE

```
% Antenna Pattern File Generation for a x pol circular aperture of
radius a
% Aperture is in the x-y plane and beam is in the z direction
close all;
clc;
clear;
fr=2400e6;
lamda = 3*10^8/fr;
HPBW = 60; % in degrees
a = 58.4 * lamda / (2*HPBW); % Uniform Circular Aperature Size (radius)
beta = 2*pi/lamda;
E0 = 1;
c = j*beta*E0*pi*a^2/(2*pi); %Contant term in E field
Directivity = (4*pi*pi*a^2)/lamda^2;
Directivity_dB = 10*log10(Directivity);
disp(['Computing pattern for HPBW = ',num2str(HPBW),' deg, f =
',num2str(fr/1e6),' MHz'])
step1 = 90; % Vertical Steps
step2 = 180; % Horizontal Steps
d_theta = 180/(step1);
d_phi = 360/(step2);
k = 0;
ip = 0;
iq = 0;
for phi = 0:d_phi:360
for theta = 0:d_theta:180 % plots out the zero point
k = k+1;
arg=beta*a*sin(theta*pi/180);
f = 1;
if abs(arg)>=1e-4
f = 2*besselj(1,arg)/arg;
end
e_theta = cos(phi*pi/180)*c*f;
e_phi = -sin(phi*pi/180)*cos(theta*pi/180)*c*f;
if theta > 90  % pattern in the rear hemisphere is zero
e_theta = 0;
e_phi = 0;
end
if phi == 0   % E-plane pattern
ip = ip + 1;
et0(ip) = 20*log10(abs(e_theta)+1e-10);
ep0(ip) = 20*log10(abs(e_phi)+1e-10);
```

```
eth0(ip) = theta;
end
if phi == 90  % H-plane pattern
iq = iq + 1;
et90(iq) = 20*log10(abs(e_theta)+1e-10);
ep90(iq) = 20*log10(abs(e_phi)+1e-10);
eth90(iq) = theta;
end
A(k,1:4) = [real(e_theta), imag(e_theta), real(e_phi), imag(e_phi)];
end
end
A0=max(max(abs(A)));
Amax=max(max(20*log10(abs(A)+1e-10)));
figure(1)
plot(eth0,et0-Amax,eth0,ep0-Amax)
title('Normalized Antenna Pattern (HPBW=90 degrees), \phi=0^o')
xlabel('Angle [degree]')
ylabel('Relative Power [dB]')
grid, legend('E-theta','E-phi')
axis([0,180,-50,0])
figure(2)
plot(eth90,et90-Amax,eth90,ep90-Amax)
title('Normalized Antenna Pattern (HPBW=90 degrees), \phi=90^o')
xlabel('Angle [degree]')
ylabel('Relative Pattern, dB')
grid, legend('E-theta','E-phi')
axis([0,180,-50,0])
% write the antenna file
fname=input('Enter the output file name with any extension: ','s');
fid=fopen(fname,'w');
S=['# Antenna file, HPBW=',num2str(HPBW),',
D=',num2str(Directivity_dB),...
    ', f=',num2str(fr/1e6),' MHz'];
fprintf(fid,'%s\n',S);
 fprintf(fid,'%s\n','rect');
 fprintf(fid,'%s\n','theta_phi');
 fprintf(fid,'%s\n','vert_first');
  fprintf(fid,'%s\n','renorm');
  fprintf(fid,'%s\n',['steps ',num2str(step1),'  ',num2str(step2)]);
  for i=1:k
   fprintf(fid,'%10.6f\t%10.6f\t%10.6f\t%10.6f\n',A(i,1:4)/A0);
end
  fclose(fid);
  disp(['File ',fname,' written'])
```

B. FIELD FILE.

```
% plot Urbana field file (surface plot only)
clear
% load file
name=input('Enter root name of the file (without .field): ','s');
fname=[name,'.field'];
fid=fopen(fname);
```

```
% discard first 6 lines (comments and headings)
for i=1:6, linedat=fgetl(fid); end
irow=0;
% read edge data in blocks
disp('reading input file .....')
n=1;
while feof(fid)==0
         irow=irow+1;
         linedat=fgetl(fid);
         B=sscanf(linedat,'%f');
         A(irow,1:11)=transpose(B);
% display every 1000 rows to monitor rate
         if floor(irow/n/5000)==irow/n/5000
             n=n+1;
             disp(['up to row ',num2str(irow)])
         end
end
disp(['data read, number of rows =',num2str(irow)])
x=A(:,2); xmax=max(x); xmin=min(x);
y=A(:,3); ymax=max(y); ymin=min(y);
z=A(:,4); zmax=max(z); zmin=min(z);
f1=A(:,5);
disp(['frequency=',num2str(f1(1))])
% find the cell size -- assumed square and
for i=2:irow
    if x(i) ~= x(i-1), dx=abs(x(i)-x(i-1)); break, end
end
disp(['cell size=',num2str(dx)])
Ex1=A(:,6)+j*A(:,7);
Ey1=A(:,8)+j*A(:,9);
Ez1=A(:,10)+j*A(:,11);
%
Emag=sqrt(abs(Ex1.^conj(Ex1))+abs(Ey1.^conj(Ey1))+abs(Ez1.^conj(Ez1)));
Emag=abs(Ez1);  % only want vertical component
Edbm=20*log10(Emag);
iprt=1;
if iprt==1   % print the field values
    disp('   x    y    z    |E|, dBm')
    for i=1:irow
    disp(['  ',num2str(x(i)),'   ',num2str(y(i)),'   ',num2str(z(i)),'
', num2str(Edbm(i))])
    end
end
hf = figure(1); clf
% set floor and ceiling values (max and min for colorbar)
Efloor=min(Edbm);  %-50;
Eceil=max(Edbm);   %20;
% add mini-patches at the corners to set the scale
% Edbm(1)=Efloor; Edbm(irow)=Eceil;
for i=1:irow
  x1=x(i)-dx/2; x2=x(i)+dx/2;
  y1=y(i)-dx/2; y2=y(i)+dx/2;
  if Edbm(i)<Efloor, Edbm(i)=Efloor; end
  if Edbm(i)>Eceil, Edbm(i)=Eceil; end
  hs2=patch([x1 x2 x2 x1],[y1 y1 y2 y2],Edbm(i));
```

```
  set(hs2,'edgecolor','none');

end
%  lighting gouraud
%  camlight

   view(0,90)

 Lx=xmax-xmin; Lxave=(xmax+xmin)/2;
 Ly=ymax-ymin; Lyave=(ymax+ymin)/2;
 Lz=zmax-zmin;
 L=max([Lx,Ly,Lz]);
 axis([Lxave-L/2,Lxave+L/2,Lyave-L/2,Lyave+L/2,0,L])
    xlabel('x, inches')
    ylabel('y, inches')
    zlabel('Height, inches')
%   title(['Observation height: ',num2str(z1(1,1)),' inches; Antenna
location = +'])
   colorbar('vert')
   grid off
```

LIST OF REFERENCES

[1] Byrum, Bruce, *Naval Forces*, Vol. 22, Issue 2, p. 50, Aldershot: 2001.

[2] Wall, Robert, Aviation Week & Space Technology, Vol. 165, Issue 5, p. 33, New York: July 31, 2006.

[3] Sumagasay, P. P., "*Vulnerability of WLANs to Interception*," Master's Thesis, Naval Postgraduate School, Monterey, California, September 2002.

[4] Boukraa, Lotfi "*Simulation of Wireless Propagation in a High-Rise Building*," Master's Thesis, Naval Postgraduate School, Monterey, California, December 2004.

[5] Kaya, Yildirim "*Simulation of Wireless Propagation and Jamming in a High-Rise Building*," Master's Thesis, Naval Postgraduate School, Monterey, California, September 2005.

[6] Pala, F., *"Frequency and Polarization Diversity Simulations for Urban UAVCommunication and Data Links*,*"* Master's Thesis, Naval Postgraduate School,Monterey, September 2004.

[7] Loke, Yong, *"Sensor Synchronization,Geolocation and Wireless Communication in a Shipboard Opportunistic Array,"* Master's Thesis, Naval Postgraduate School, Monterey, July 2006.

[8] Ulama, Tuncay, *"Frequency And Polarization Diversity Jamming of Communications in Urban Environments*,*"* Master's Thesis, Naval Postgraduate School, Monterey, September 2005.

[9] Siwiak, K., *Radiowave Propagation and Antennas for Personal Communications,* 2nd Edition, Artech House, Inc., Norwood, Massachusetts, 1998.

[10] Jenn, D. C., *Radar and Laser Cross Section Engineering*, American Institute of Aeronautics, Washington, 1995.

[11] Jenn, D. C., *Lecture Notes for EC3630 (Radio wave Propagation)*, Naval Postgraduate School, 2004 (unpublished).

[12] Harney, B., *Notes for TS3000 (Combat Systems)*, Naval Postgraduate School, 2004 (unpublished).

[13] Stutzman W. L., and Thiele, G.A., *Antenna Theory and Design*, 2nd Edition, John Wiley & Sons, Inc., Hoboken, New Jersey, 1998.

[14] *Urbana* 3-D Wireless Toolkit, http://www.saic.com/products/software/urbana/, last accessed July 2006.

[15] Wikipedia web site, http://en.wikipedia.org, last accessed July 2006.

[16] 3D CAD Browser, http://www.3dcadbrowser.com/, last accessed August 2006.

[17] CUBIT 10.1 User Documentation, http://cubit.sandia.gov/help-version10.1/importing_and_exporting_data/geometry_import/importing_facet.htm, last accessed July 2006.

[18] Lindell, I.V., Sihvola, A.H., "*Method for problems involving perfect electromagnetic conductor (PEMC) structures*," *IEEE Transactions on Antennas and Propagation,* Volume: 53, Issue: 9, pp. 3005–3011, September 2005.

INITIAL DISTRIBUTION LIST

1. Defense Technical Information Center
   Ft. Belvoir, Virginia

2. Dudley Knox Library
   Naval Postgraduate School
   Monterey, California

3. Professor David C. Jenn
   Department of Electrical and Computer Engineering
   Naval Postgraduate School
   Monterey, California

4. Professor Michael A. Morgan
   Department of Electrical and Computer Engineering
   Naval Postgraduate School
   Monterey, California